Exploring the Ub/UBL landscape with activity-based probes

Witting, K.F.

Chapter 3

A cascading activity-based probe sequentially targets E1-E2-E3 Ubiquitin enzymes

Monique P.C. Mulder*, Katharina Witting*, Ilana Berlin*, Jonathan N. Pruneda, Kuen-Phon Wu, Jer Gung Chang, Remco Merkx, Johanna Bialas, Marcus Groettrup, Alfred C.O. Vertegaal, Brenda A. Schulman, David Komander, Jacques Neefjes, Farid El Oualid, and Huib Ovaa, *Nat. Chem. Biol.* 2016, 12(7), 523-30.

*Authors contributed equally

Abstract

Post-translational modifications of proteins with Ubiquitin (Ub) and Ubiquitin-like (Ubl) modifiers, orchestrated by a cascade of specialized E1, E2 and E3 enzymes, control a staggering breadth of cellular processes. To monitor catalysis along these complex reaction pathways, we developed a cascading activity-based probe, UbDha. Akin to the native Ub, upon ATP-dependent activation by the E1, UbDha can travel downstream to the E2 (and subsequently E3) enzymes through sequential trans-thioesterifications. Unlike the native Ub, at each step along the cascade UbDha has the option to react irreversibly with active site cysteine residues of target enzymes, thus enabling their detection. We show that our cascading probe 'hops' and 'traps' catalytically active Ubiquitin-modifying enzymes (but not their substrates) by a mechanism diversifiable to Ubls. Our founder methodology, amenable to structural studies, proteome-wide profiling and monitoring of enzymatic activities in living cells, presents novel and versatile tools to interrogate the Ub/Ubl cascades.

Introduction

Post-translational modifications of cellular targets with Ubiquitin (Ub) or Ubiquitin-like (Ubl) modules are potent regulators of protein function and thus govern a wide range of biological processes[1]. While the general biochemical logistics of Ub/Ubl activation, conjugation and ligation, orchestrated sequentially by the E1, E2, and E3 enzymes, are highly conserved among eukaryotes, the number and flavour of individual players in each organism's relevant enzymatic repertoire can differ widely[1]. Humans are known to harbour 2 E1, ~30 E2s and ~600 E3s in the Ub conjugation cascade, and while some are highly specific for certain targets, others appear relatively promiscuous. The sheer complexity of such enzymatic networks, further inundated by ~80 specific proteases responsible for removal of these modifications[1], enables highly specialized and sensitive modes of regulation, necessary to accommodate dynamic cellular events. On the flip side, deregulation of these pathways is a common feature in cancer, neurodegenerative, and inflammatory diseases. Similarly, some pathogens have evolved to perturb or exploit the host's Ub/Ubl conjugation cascades to their advantage[2]. Despite their importance, development of comprehensive tools to assess the enzymology of these processes has been a long-standing roadblock in the field.

An important class of reagents used to study enzymatic activity, structure and substrate specificity within the Ub/Ubl modification system are activity-based probes (ABPs)[3,4]. In the last decade, we and others have developed various ABPs for deubiquitylating enzymes (DUBs) and Ubl specific proteases[5-7]. Among the advantages of such probes is their ability to report on DUB activities in cellular extracts and even intact cells, thus facilitating the study of these enzymes in their biological context[8]. Development of analogous tools for the ligation machinery has proven challenging. Unlike DUBs, which contain highly reactive cysteine (Cys) nucleophiles, ligases possess less nucleophilic active site Cys residues, rendering them more difficult to trap with electrophiles. Recently, Ubl-AMP probes were reported to selectively label cognate activating enzymes[9-12]. However, because ligation requires transfer of Ub/Ubl between enzymes, the challenge of monitoring reactions throughout the cascade remained. To tackle this, we developed a mechanism-based ligase probe that undergoes sequential trans-thioesterification reactions as it cascades from the E1 to the E2 and subsequently the E3 stage. In addition, at each step of the cascade our probe has the option to irreversibly trap the active site Cys residues of the enzymes in question. This methodology, implemented and characterized using the Ub-specific conjugation machinery, is further extended to the NEDD8 enzyme family, demonstrating general applicability of our probe design to Ubls.

The unique properties of our cascading probe enable direct monitoring of sequential E1, E2, and (HECT) E3 activities in a wide variety of experimental settings. Given the ATP-dependence of its reactivity against ligases, combined with its lack of transfer to substrates, our probe is well suited for proteome-wide profiling of relevant enzymatic cascades. Furthermore, upon

introduction into living cells, our probe monitors enzymatic activities of interest and reports on changes in response to chemical or genetic inhibition. From the structural perspective, our stable mechanism-based trapping of catalytic Cys residues circumvents potential disadvantages incurred by traditional methods of stable E2-Ub conjugate preparation requiring active site mutagenesis[13-17]. Collectively, these novel features of our ABP tool present previously inaccessible avenues for targeting and monitoring enzymatic activities along the Ub/Ubl conjugation cascades, with implications for drug discovery and cell as well as structural biology of these pathways.

Results

Design and synthesis of the cascading ABP

To initiate the Ub/Ubl modification cascade, the E1 activating enzyme adenylates the C-terminus of Ub at the expense of ATP, which results in a high energy E1~Ub thioester formed upon an intramolecular reaction of the intermediate adenylate with the E1 active site Cys nucleophile. Next, a trans-thioesterification reaction transfers the activated Ub to a conserved E2 Cys, thus forming an E2~Ub thioester intermediate, which subsequently enables transfer of Ub onto a substrate with the help of an E3[18]. It is known that a Ub-G76A mutant can also be processed by the E1-E2-E3 cascade, albeit with reduced efficacy[19,20]. We reasoned that replacing the C-terminal alanine by a latent and electrophilic dehydroalanine (Dha) moiety, would retain recognition by the E1-E2-E3 enzymes, allowing the UbGly76Dha (UbDha) to traverse the cascade (Fig. 1). Analogous to Ubiquitin activation, UbDha is activated by the E1 enzyme through the formation of an adenylate intermediate, which strongly increases the electrophilic character of the Michael acceptor (Dha moiety). The activated methylene group of the Dha moiety is now poised to *either* covalently trap the enzyme in an E1-UbDha thioether adduct (Fig. 1, pathway a) *or follow* the native ligation route resulting in an E1~UbDha thioester (pathway b). In the second scenario, UbDha is available for transfer to an E2 enzyme, during which an analogous two options of covalent thioether adduct with the probe (pathway a) or a native trans-thioesterification reaction (pathway b) arise. Lastly, similar options apply to the subsequent transfer of UbDha from the E2 to an active site cysteine-dependent E3 enzyme (i.e. from the HECT or RBR families of E3 ligases[21]).

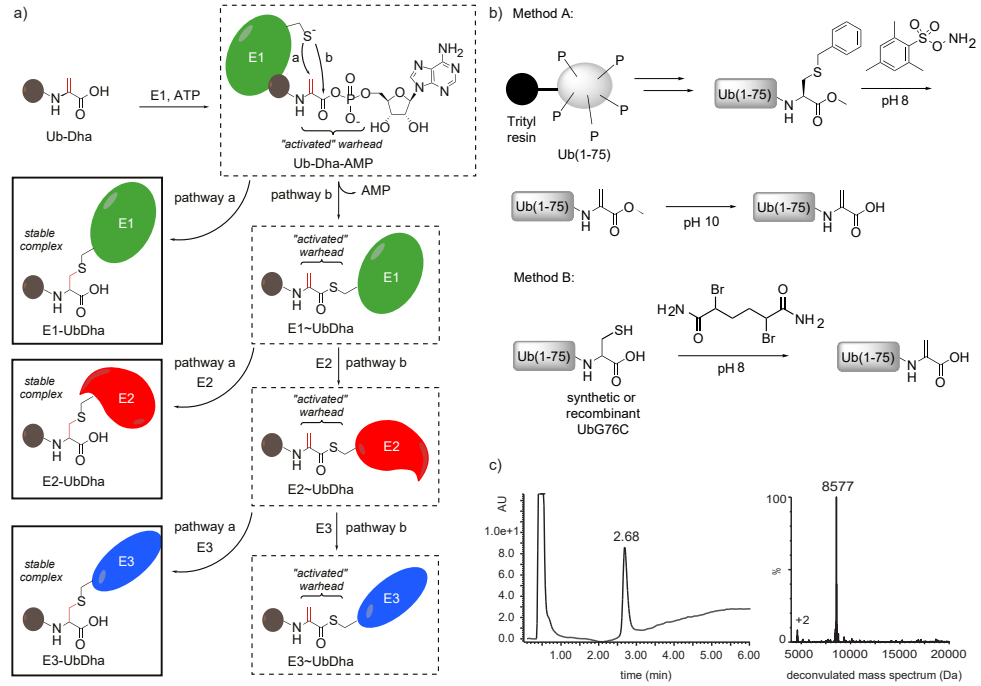

Figure 1 | Mechanism and synthesis of the activity based probe Ub-Dha. *In situ* activation of Ub-Dha with E1 and ATP results in a mechanism based ABP for E1, E2 and Cys dependent E3 enzymes. Pathway a describes the covalent trapping of the enzyme (E-UbDha = thioether-linked adduct), while pathway b depicts the native transthioesterification processing of the probe (E~UbDha = thioester intermediate of conjugate) by the cascade.

UbDha was synthesized starting from Ub(1-75) (Supplementary results, Supplementary Fig. 1), using our previously reported linear Fmoc-based solid phase synthesis (SPPS) of Ub[22], where coupling H-Cys(Bn)-OMe to the C-terminal carboxyl group of protected Ub(1-75) afforded Ub(1-75)-Cys(Bn)-OMe. This was subsequently transformed into UbDha-OMe by oxidative elimination with O-mesitylenesulfonylhydroxyl-amine (MSH)[23]. Finally, the methyl ester was hydrolysed, to generate the UbDha probe. We also used the recently reported 2,5-dibromohexanediamide reagent to convert a Cys into a Dha moiety (Supplementary Fig. 1; Method B)[23,24]. Importantly, in contrast to MSH, 2,5-dibromohexanediamide reacts with a C-terminal Cys residue and thus allows the use of recombinant Ubl G76C mutants to prepare probes.

Covalent bond formation with conjugating enzymes

To evaluate the ability of our probe to travel the cascade, we began by subjecting the Ub-activating UBE1 enzyme to UbDha *in vitro*. SDS-PAGE analysis of the reaction revealed

formation of an UBE1-UbDha adduct (Fig. 2a), consistent with a thioether linkage due to its stability under reducing conditions. ATP-dependence of the reaction indicated that the ligation proceeds through the adenylate intermediate (Fig. 1). Similar observations were made for UBA6 (Fig. 2a, right panel), the second Ub E1 enzyme, which also activates the Ubl modifier FAT10[25]. To test whether the E1-UbDha thioester can transfer UbDha to the E2 stage, we added UBE2L3 to the reaction in Fig. 2a. Whereas SDS-PAGE analysis under non-reducing conditions facilitated labeling with both native Ub and UbDha (Fig. 2b), under reducing conditions only the UbDha probe was able to form a stable adduct with the E2 enzyme. As expected, labeling was not observed in the absence of ATP (Supplementary Fig. 2). Interestingly, the double UbDha loaded UBE1 intermediate[26] (Supplementary Figs. 2 and 3) observed in the absence of an E2, was sensitive to co-incubation with UBE2L3 (Supplementary Fig. 4), while adding UBE2L3 subsequent to UBE1 labeling with UbDha had no effect in this context. This may indicate a transfer of Ub from the adenylation active site to a nearby Cys in the adenylation domain of UBE1, which simply does not occur when UbDha is quickly transferred to the next step in the cascade, here transfer to E2[27]. In addition to UBE2L3, UbDha showed labeling of 26 other Ubiquitin E2s (Supplementary Fig. 5), but remained unreactive against Ubl E2s (UBE2F, UBE2I, UBE2L6 and UBE2M). UbDha was also unable to label the Ub E2 UBE2Z downstream of UBE1 due to the enzyme's selectivity for the alternative E1, UBA6[25]. Noncanonical catalytically inactive E2s UBE2V1 and UBE2V228 with scaffolding function also failed to react with the probe (Supplementary Fig. 5). Collectively, these results demonstrate broad utility of the UbDha probe in monitoring mechanism-based transfer of activated Ub from the E1 to a wide range of cognate E2s. Under non-reducing conditions, (Fig. 2b, Supplementary Fig. 6) a ternary complex of E1~UbDha-E2 was revealed. Here, the acceptor E2 enzyme reacts directly with the Michael acceptor on the probe-donating E1-thioester adduct. This third pathway of probe action (Supplementary Fig. 6, right panels) was further confirmed by the stable oxyester linked E1-O~UbDha adduct (Supplementary Fig. 6).

Next, we investigated whether UbDha could be further delivered to an E3, bearing an active site Cys. The family of E3 ligases is subdivided into three major classes according to their mechanism of action[21]. In humans, the known thioester-forming E3s, which harbor catalytic Cys residues loaded with Ub by a mechanism analogous to the E1 and E2 enzymes, fall into the HECT (homologous to E6-AP terminus, 28 family members in humans) and RBR (RING-between-RING, 13 members in humans) classes. In contrast, the RING E3 ligases act as scaffolds between the E2~Ub thioester and the substrate protein, but do not themselves form thioesters[21]. We therefore examined a well-characterized HECT E3 ligase NEDD4L14. As expected, a Cy5-UbDha-NEDD4L thioether adduct was observed downstream of UBE1 and UBE2L3 (Fig. 2c). Similarly, a panel of 9 other HECT E3s also reacted with the probe (Supplementary Fig. 7). Because NEDD4L initially showed reactivity without ATP (Supplementary Fig. 7), we repeated this experiment with an active site Cys-

to-Ala mutant and a mutant in which the four non-catalytic Cys residues were mutated to Ala (Supplementary Fig. 8). Labeling was clearly visible under standard assay conditions, whereas omitting either ATP, UBE1, and UBE2D2 or ATP alone resulted in virtually no labeling. Interestingly, the catalytic Cys-to-Ala mutant showed reduced but not completely abolished labeling compared to the wild-type NEDD4L. A similar observation was made for the non-catalytic 4x Cys-to-Ala mutant, suggesting that NEDD4L has at least two cysteines competent to receive an activated UbDha. Not all HECT E3s have a Cys adjacent to a noncovalent Ub-binding site. For instance, the HECT domain of Smurf2 (54% identical to NEDD4L) lacks the candidate Cys in the noncovalent Ub binding site and showed no alternative labeling of any of its six non-catalytic Cys residues with our probe (Supplementary Fig. 9).

For a native Ub, the next step in the cascade following reactivity with an E3 would result in ligation to a target substrate. To test whether our probe behaves similarly, we chose WBP229 a known substrate for the UbDha-reactive E3 HECT ligases (NEDD4L, Rsp5, WWP1 and WWP2). While incubation with Ub showed multiple turnover Ubiquitination on WBP2, no Ubiquitination was observed using UbDha even with prolonged reaction times (Fig. 2d and Supplementary Fig. 10). This feature makes UbDha particularly advantageous for enzymatic profiling in cellular systems, where irrespective of the presence of substrates, our activated warheads will remain on the active enzymes themselves.

Generalizing the cascading ABP methodology to Ubls

To show that our probe design is applicable beyond the Ub cascade, we synthesized the NEDD8 G76C mutant by linear Fmoc based solid phase synthesis (SPPS)[30] and easily transformed the Cys into Dha by overnight incubation with 2,5-dibromohexanediamide. Following incubation of NEDD8Dha with UBA3/NAE1, SDS-PAGE analysis revealed formation of the expected UBA3-NEDD8 thioether adduct and a double NEDD8-loaded UBA3 adduct[31] (Supplementary Fig. 11 and Supplementary Fig. 12). Co-incubation with UBE2M resulted in the formation of a NEDD8-UBE2M thioether adduct (Supplementary Fig. 11). As with the Ub E1 UBE1, formation of double NEDD8Dha-linked UBA3 was suppressed when UBE2M was present during the E1 labeling. Similarly, treatment with 2-mercaptoethanol had no effect on adduct formation, and labeling with NEDD8Dha failed in the absence of ATP (Supplementary Fig. 11). These experiments demonstrate that our founder cascading ABP design can be extended to other Ubl modification cascades.

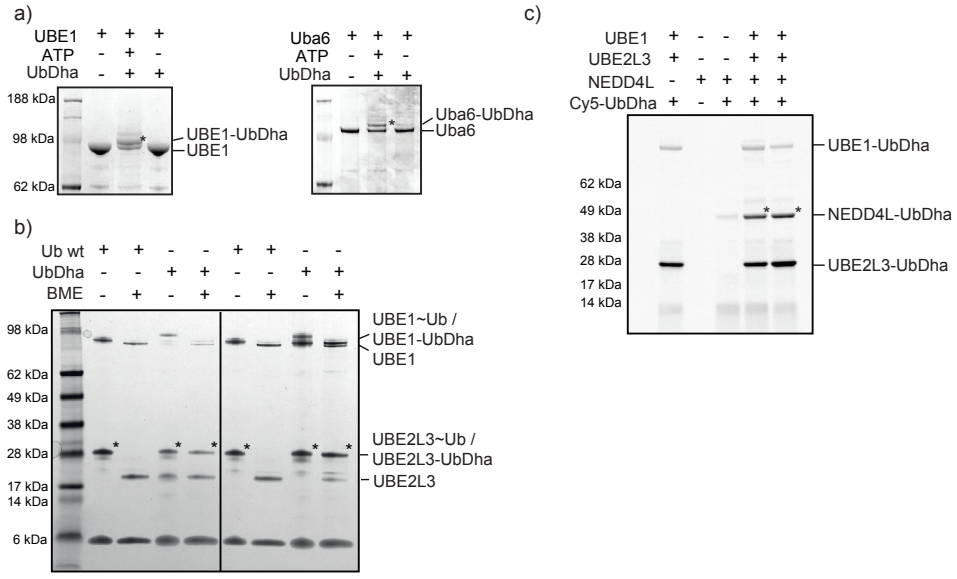

Figure 2| a) ATP-dependent labeling of UBE1 (left) and UBA6 (right). (b) Reactivity of UBE2L3 toward Ub and UbDha under reducing and nonreducing conditions. (c) Fluorescence scan showing NEDD4L HECT labeling with Cy5–UbDha. (d) Multiple-turnover Ubiquitination on substrate WBP2 does not occur with UbDha. Asterisks in a and b indicate modified forms of UBE1, UBA6, UBE2L3 and NEDD4L.

Structure determination of a thioether-linked E2-Ub adduct

To evaluate the structural integrity of our thioether-linked adducts we performed both solution-based and crystallographic studies. Solution properties of the oxyester-linked UBE2N-O~Ub conjugate (in which the active site Cys has been mutated to Ser) have been thoroughly characterized by NMR spectroscopy and small angle X-ray scattering[32], allowing us to validate the analogous thioether linkage as a suitable mimic. Analysis of chemical shift perturbations in the 1H,15N HSQC spectrum of UBE2N (Supplementary Fig. 13) arising from conjugation with Ub revealed several regions affected in both the thioether- and oxyester-linked samples (Fig. 3a; compare red to black) localized primarily to Loop 3, Helix 2, Loop 8, and the penultimate C-terminal helix (Fig. 3b, red surfaces). These perturbed regions can be attributed to the "closed" conformation of the UBE2N-UbDha thioether adduct, which is predominant in solution[32] and indicates the overall behavior of the thioether-linked adduct to be similar to the oxyester linkage. Certain resonances in the UBE2N-UbDha HSQC spectrum displayed markedly different characteristics from the oxyester-linked sample (Fig. 3a), mapped to the region directly surrounding the active site (Fig. 3b, blue surfaces). Given the exquisite sensitivity of amide resonances to their local chemical environment, such differences between the two linkage types are most likely due to their differing chemical

properties, and not to a larger structural change.

While solution studies indicate normal inter-domain behavior within the thioether-linked adduct, they lack the atomic resolution of the linkage and the surrounding active site residues. To remedy this we crystallized the UBE2D3-UbDha adduct under conditions published for the oxyester-linked UBE2D3-O~Ub conjugate[33]. The 2.2Å UBE2D3-UbDha thioether structure was strikingly similar to the published oxyester structure (PDB 3UGB), with Cα RMSD values of 0.23 and 0.35Å for UBE2D3 and Ub, respectively (Fig. 3c, Supplementary Table 1). The only significant deviation between the two structures was found in the Ub C-terminus near the linkage itself, manifested in an RMSD of 1.13Å for Ub residues 73-76. The thioether linkage was readily revealed in the corresponding electron density (Fig. 3d), although detailed features of the omit map did suffer from high B factors in the flexible Ub C-terminus (average B-factor of 105.7 for Ub residues 75-76 compared to 49.4 for all protein). Nearby residues within the UBE2D3 active site were found to adopt nearly identical conformations, with the only exception being Arg90, which was missing from the electron density (Fig. 3e). An overlay of the oxyester and thioether structures suggests that the additional carboxylate group of the thioether linkage could displace the Arg side chain from the E2 active site cleft, although to our knowledge there is currently no known role for this residue in E2 catalysis.
Preparation of stable E2-Ub conjugates has in the past relied on the DCA method[13], oxyester[14-16], and isopeptide[17] bonds, all necessitating mutations to the enzyme's active site. Furthermore, oxyester-linked E2~O-Ub/ E2~O-Ubl conjugates suffer from susceptibility to hydrolysis, particularly in the presence of an active E3 ligase[14-16], thereby limiting their use in structural applications and preventing any potential utility in cell-based studies. In contrast, UBE2D3-UbDha and UBE2N-UbDha thioether-linked adducts remained inert in the presence of activating factors, such as the E3 ligases TRAF6 (RING-type) or NEDD4L (HECT-type), or an accessory E2-variant UBE2V2 with or without TRAF6, respectively (Figs. 3f and 3g). As a catalytically inert mimic of native thioester-linked conjugates, the thioether-linked adduct behaved as a competitive inhibitor of the ligation machinery in single-turnover assays monitoring diUb formation by UBE2N, UBE2V2, and the E3 ligase cIAP (Supplementary Fig. 14).

Combined with solution and crystallographic data, these functional assays support the utility of thioether-linked E2-UbDha adducts as stable mimics in both structural and functional studies.

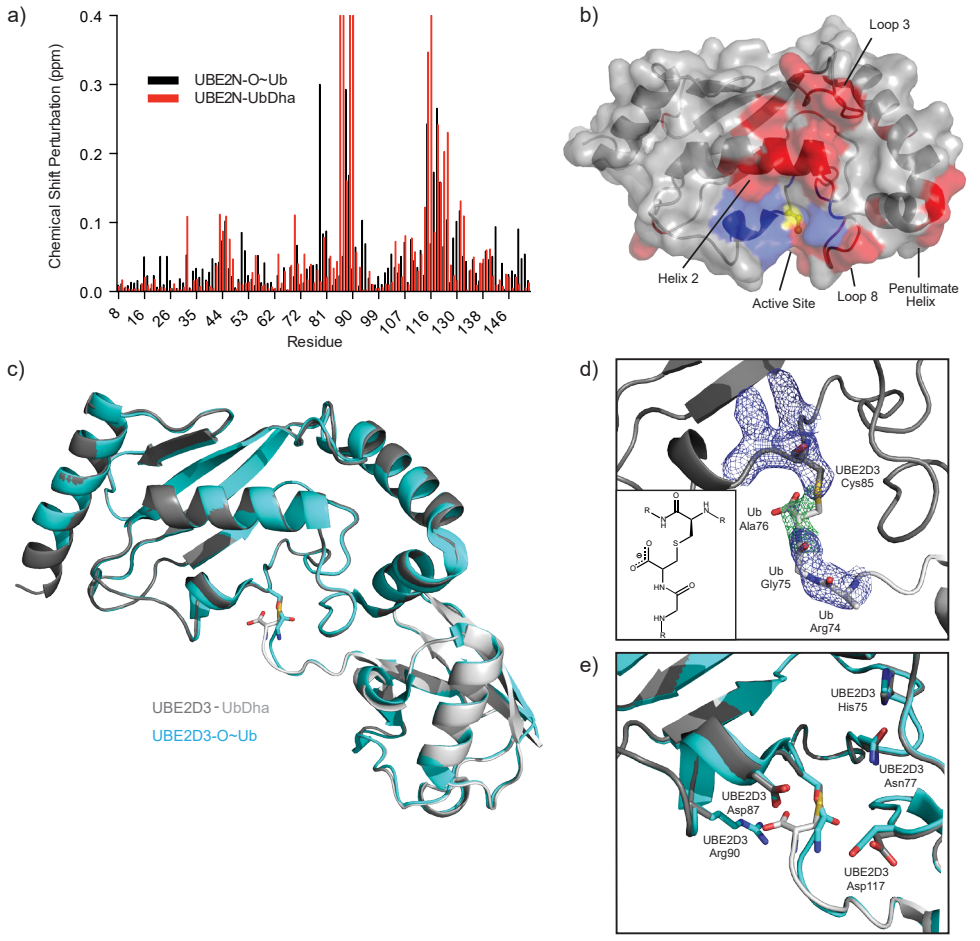

Figure 3 | Structural studies of thioether-linked E2-Ub adducts. a) UBE2N chemical shift perturbations upon Ub activation for oxyester (black) and thioether (red) linkages. Resonances perturbed beyond facile re-assignment were plotted using maximum perturbation value. b) Changes (from a) mapped onto the UBE2N structure (PDB 1J7D) (similarities in red; differences in blue).

Figure 3 | *continued* Active site Cys is colored yellow. c) Superposition of thioether-linked UBE2D3-UbDha conjugate (gray) over the oxyester-linked form (cyan, PDB 3UGB). d) Simulated annealing omit map of electron density surrounding the thioether linkage. 2|Fo|-|Fc| electron density (blue) contoured at 1σ, |Fo|-|Fc| density (green) contoured at 3σ. Inlay: diagram illustrating the thioether linkage. e) Overlay of E2 active site residues in thioether (gray) and oxyester (cyan) structures. Stability of the thioether-linked UBE2D3- and UBE2N-UbDHA adducts, incubated with f) RING E3 ligase TRAF6 or the HECT E3 ligase NEDD4, or g) accessory E2-variant UBE2V2, alone or in combination with the RING E3 ligase TRAF6.

UbDha probe as a proteomics tool

Having validated activity and structural integrity of the UbDha probe, we turned to enzymatic cascade profiling in biological samples. Incubation of cell extracts with Cy5-UbDha revealed robust labeling of both UBE1 (Fig. 4a) and UBA6 activating enzymes, reliably abrogated by apyrase treatment (Supplementary Fig. 15). Appearance of additional ATP-dependent bands was also detected on the same timescale, (Supplementary Fig. 15), supporting the *in vitro* data that the probe is passed downstream. To identify these proteins, we utilized the biotin-labeled probe variant for affinity-based proteomic profiling[3] of human cervical cancer (HeLa, Fig. 4b) and melanoma (MelJuSo, Supplementary Fig. 16) cell extracts. We used the ATP-dependent reactivity of our probe to our advantage and performed affinity-based proteomic profiling in the presence of ATP, as compared to apyrase-mediated ATP-depletion. Mass spectrometric analysis of proteins associated with the probe in an ATP-dependent manner, retrieved both Ub E1 enzymes and numerous downstream E2 enzymes. Specifically, roughly half of known human E2 enzymes[34] charged by UBE1 (as well as UBE2Z, charged specifically by UBA6) were identified with high confidence in both cell lines. Among the most enriched proteins were UBE2L3, UBE2S and UBE2K, all of which can readily accept Ubiquitin from UBE1 and UBA625. Interestingly, three different members of the E2D subfamily were recovered: UBE2D2, UBE2D3 and UBE2D4, in fact the largely uncharacterized UBE2D4 was the top hit in HeLa cells (Fig. 4b). By contrast, UBE2D4 was not recovered in MelJuSo cells, exemplifying how the UbDha probe can facilitate unbiased proteome-wide comparisons of enzymatic reactivities. In addition to canonical E2s, we also detected atypical E2/E3 hybrid enzymes (UBE2O and BIRC6) as well as HECT E3s. While the E3 ligases UBE3A and HECTD1 were found in both cell lines, TRIP12 was observed only in MelJuSo cells. UBE3A prefers to accept Ub from UBE2L3[35], which was recovered in high abundance from both cell lines, indicating isolation of a full E1-E2-E3 cascade. Enzymes of interest, immunoprecipitated directly from cells, can be subsequently investigated using the UbDha probe in the presence of supplemented reaction components of choice. This is demonstrated by the ability of GFP-UBE2J1 but not GFP-UBE2Z to accept activated Cy5-UbDha from UBE1 (Fig. 4c). As expected, mutation of active site Cys 91 of GFP-UBE2J1 to Ala (C91A) abrogated labeling, demonstrating suitability of UbDha for mutational studies.

We also identified four DUBs (OTUB1, OTUD7B, UCHL3 and USP15) in pull-downs with the ligase probe (Fig. 4b and Supplemental Fig. 16). Because DUBs harbor highly reactive active site Cys residues, we assessed potential cross reactivity by incubation of the Cy5-UbDha probe with cell lysates ectopically expressing various GFP- or FLAG-tagged DUBs (Supplemental Fig. 17a) alongside the recently reported DUB-specific ABP, Cy5-UbPA[30]. While Cy5-UbPA readily modified all the active DUBs tested here, only incubation with excessive amounts of UbDha resulted in often marginal DUB labeling. Moreover, labeling of even highly reactive DUBs with Cy5-UbDha, such as OTUB1 and OTUB2 could be readily abolished by pretreatment with UbPA (Supplementary Fig. 17b). Of note, the DUBs recovered with UbDha in our proteomic experiment (particularly OTUB1) can interact with E2 enzymes[36]. Since DUB-mediated catalysis proceeds independently of ATP, recovery of these DUBs in the ATP-dependent setting can be a result of co-isolation with their active partner ligases.

Activity based protein profiling in cells

To address the efficacy of UbDha in monitoring the Ub-conjugating cascade in the cellular context, we next introduced Cy5-UbDha into HeLa cells by electroporation. In-gel fluorescence analysis followed by immunoblotting revealed speedy engagement of both human Ub activating enzymes (Fig. 5a) on a time-scale comparable to (if not faster than) that observed in lysate labeling experiments (Fig. 4a). Furthermore, treatment of cells with the UBE1 inhibitor PYR-4137 prior to introducing the probe noticeably reduced detectable UBE1 activity (Fig. 5b), indicating that the probe can be used to monitor enzymatic inhibition in living cells.

Cells harboring Cy5-UbDha were found to exhibit normal morphology, with the probe being evenly distributed throughout the nuclear and cytoplasmic space, as expected when small molecules such as Ubiquitin move unrestricted across the nuclear membrane38 (Fig. 5c, top panels). Of note, in cells undergoing late stages of cell division, accumulation of Cy5-UbDha was consistently observed at the cytokinetic bridge (Supplementary Fig. 18), consistent with the site of BIRC6 activity at this time in the cell cycle[39]. Having detected BIRC6 in high abundance in our proteome-wide active ligase analysis (Fig. 4b), these observations suggest that our probe could be used to study spatial and/or temporal aspects of relevant enzymatic cascades. For instance, introduction of Cy5-UbDha into HeLa cells ectopically expressing predominantly nuclear GFP-UBE1 resulted in the corresponding nuclear accumulation of the probe (Figs. 5c, and 5d) relative to untransfected cells. In-gel fluorescent analysis and immunoblotting of corresponding lysates confirmed formation of a GFP-UBE1-UbDha adduct (Fig. 5e).

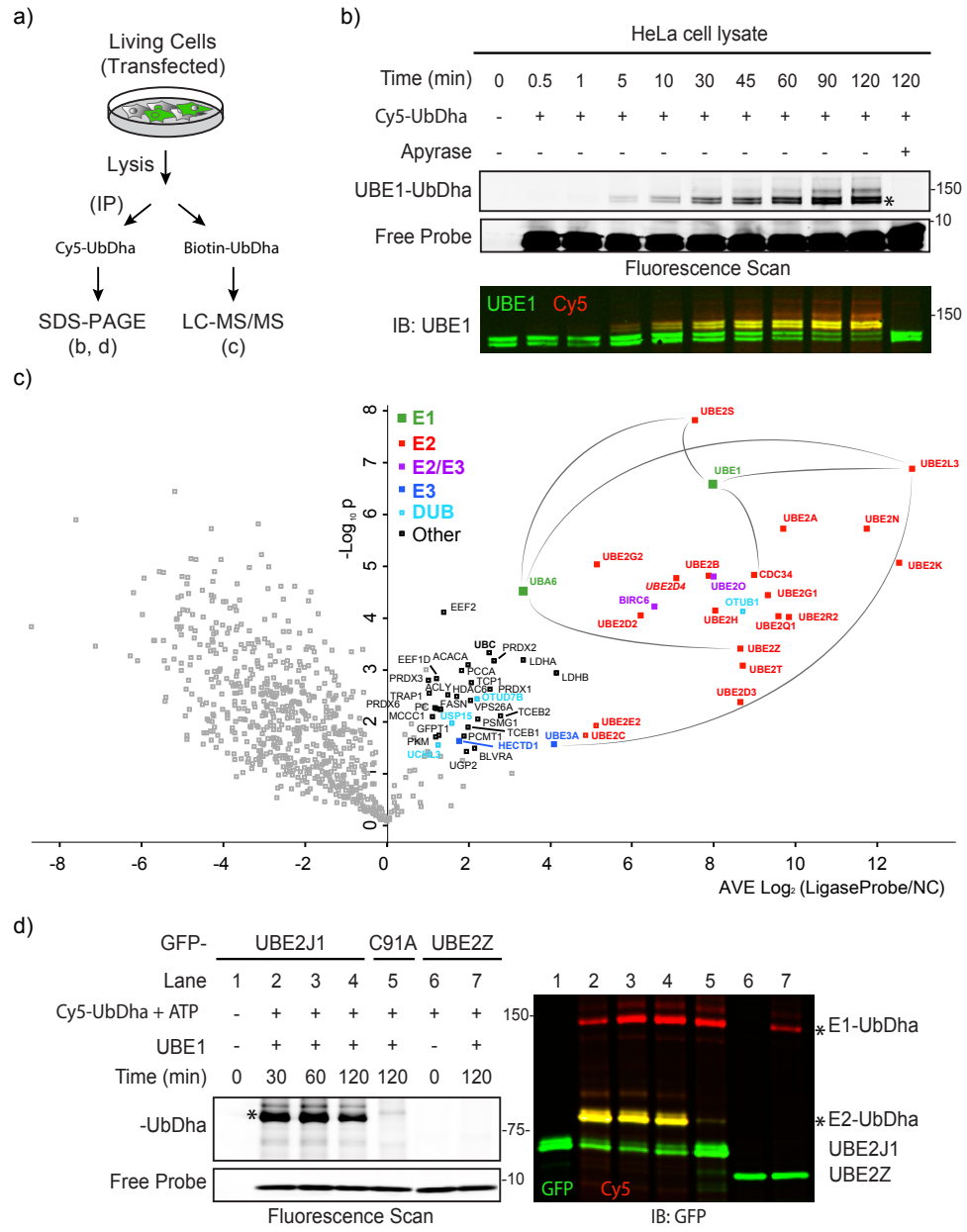

Figure 4 | Proteome-wide activity profiling of Ub-conjugation machinery. a) Time-course of UBE1 labeling in HeLa cell extracts with Cy5-UbDha in the absence (-) or presence (+) of ATP scavenger apyrase. b) Proteomic profiling of the Ub activation, conjugation and ligation machineries in HeLa cells. Volcano plot of pairwise comparison of proteins bound to the Biotin-UbDha probe relative to apyrase treatment (negative log10 p-value, y-axis) as a function of fold enrichment (average log2, x-axis). Confidently identified proteins (average log2 ratio >1, $p < 0.05$) are marked as follows: E1 (green), E2 (red), HECT E3 (blue), hybrid E2/E3 (purple) and DUBs (light blue); proteins unrelated to the Ub cycle

Figure 4 | *continued*. are marked in black, and those falling below the threshold are shown in gray. Several known cascade connections are highlighted with gray lines. c) Labeling of GFP-tagged enzymes isolated from HeLa cells (UBE2J1 or it catalytic mutant C91A versus GFP-UBE2Z) with Cy5-UbDha downstream of purified UBE1. Asterisks (*) indicate modified forms of E1 and E2 enzymes. For uncut gels, see Supplementary Figure 20.

To investigate whether the probe, while inside the cell, can be passed downstream of the E1, we introduced Cy5-UbDha into cells expressing UBE2J1 or its catalytically inactive C91A or C91S mutants. Catalysis-dependent modification of the E2 with the probe was indeed observed (Figs. 6a and 6b, left panel) and found to be sensitive to inhibition of the upstream UBE1 (Fig. 6b, right panel). UBE2J1, which we isolated with UbDha from MelJuSo cell lysates (Supplementary Fig 16), localizes to the endoplasmic reticulum (ER), where it functions in ER-associated degradation (ERAD)[40]. In cells, Cy5-UbDha was found to readily colocalize with wild type, but not catalytically dead UBE2J1 (Figs. 6c and 6d). Importantly, such colocalization was sensitive to inhibition of the upstream E1 (Figs. 6c and 6d), indicating that imaging of intact cells harboring fluorescently labeled UbDha can report on relevant enzymatic cascades. Collectively, these experiments illustrate a wide range of utilities for UbDha in the study of Ubiquitin ligase activities in cells. To the best of our knowledge, UbDha is the first probe that allows cascade-dependent profiling of Ubiquitin conjugating enzymes in a physiologically relevant setting.

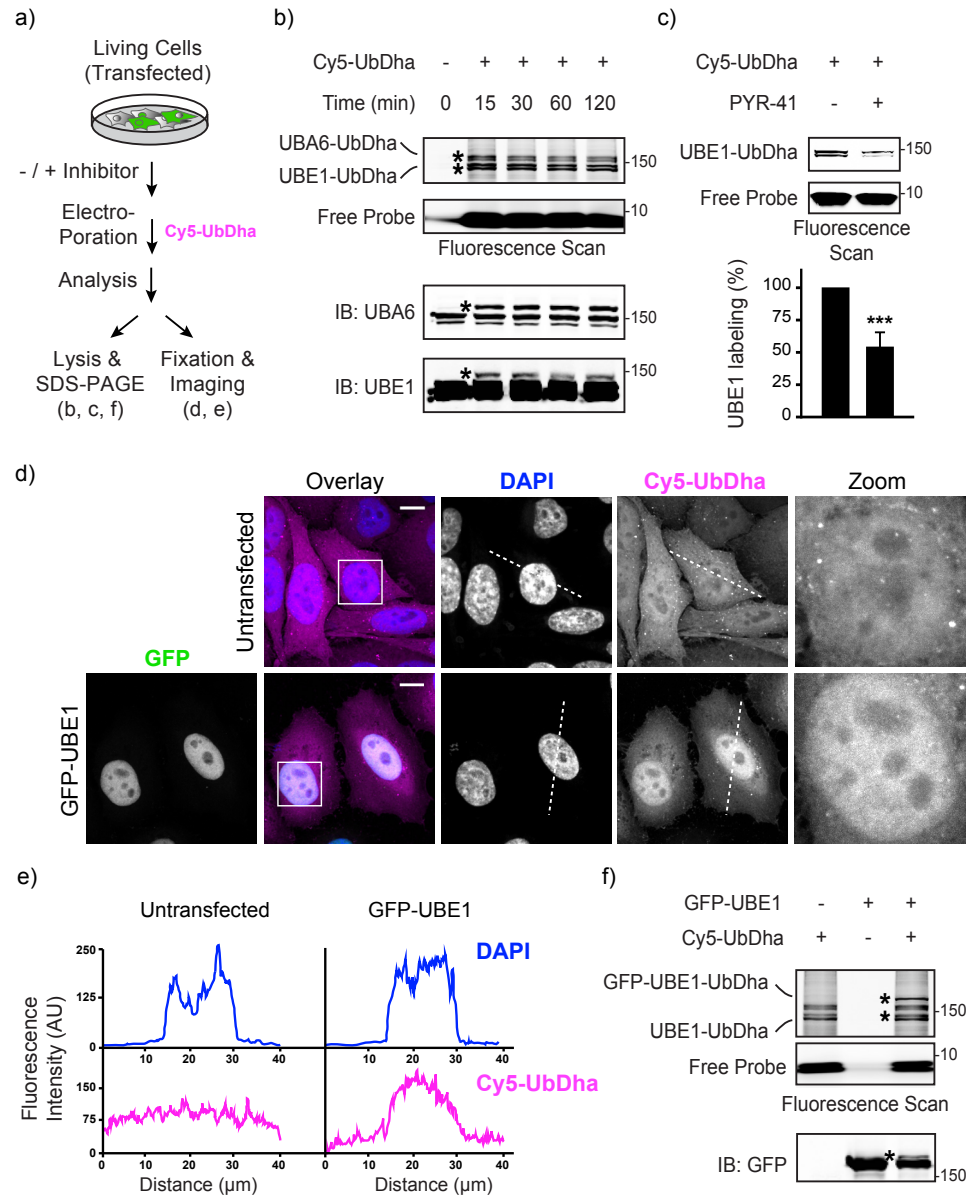

Figure 5 | Activation of UbDha *in vivo*. a) *In vivo* labeling of endogenous E1 enzymes with Cy5-UbDha. Fluorescence scanning and immunoblotting of lysates from HeLa cell electroporated with the probe and harvested at indicated time intervals following electroporation with the probe. b) *In vivo* labeling of UBE1 with Cy5-UbDha following UBE1 inhibitor PYR-41 (50 µM) treatment. Fluorescence scan and quantification (% labeling in the absence of PYR-41; n=3, error bars correspond to SD, with significance (p) assessed using a two-sided t-test) are shown. c) Distribution of Cy5-UbDha (magenta) in cells ectopically expressing GFP-UBE1 (green) relative to untransfected cells. Representative 3D confocal compilations of fixed cells treated as indicated are shown with DAPI (blue) overlays and nuclear insets;

Figure 5 | *continued.* scale bars = 10 µm. d) Pixel traces of DAPI and Cy5-UbDha (marked with dotted lines in d) plotted as fluorescence over distance. e) Formation of the GFP-UBE1-UbDha adduct in cells. Asterisks (*) indicate modified forms of E1 enzymes. For uncut gels, see Supplementary Figure 21.

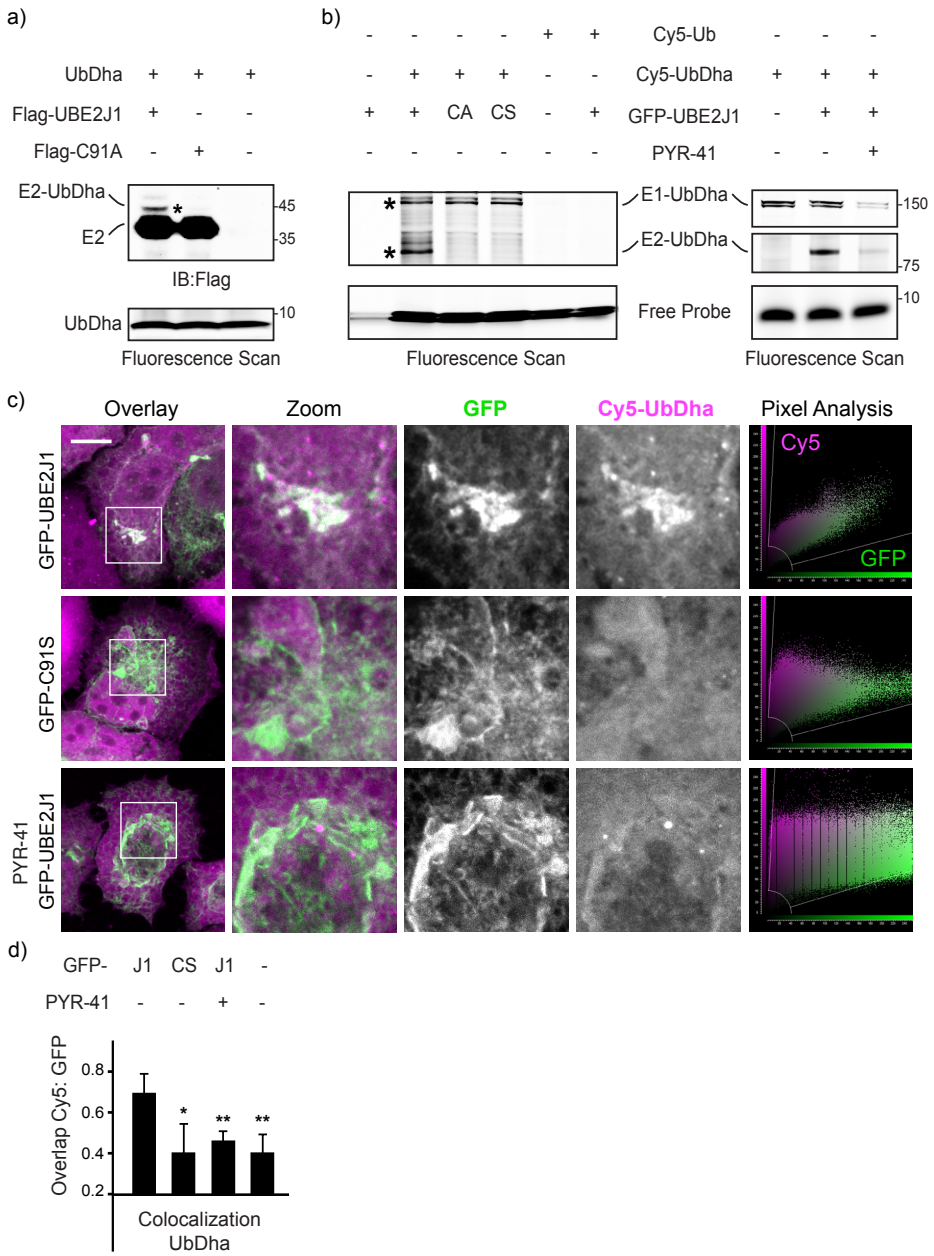

Figure 6 | Probing *in vivo* E1-E2 cascade with UbDha. a) *In vivo* UbDha adduct formation with Flag-UBE2J1 versus its catalytic mutant C91A by immunoblot against Flag. b) Reactivity of GFP-UBE2J1 versus its mutants C91A or C91S (left panel) or as a function of UBE1 inhibition (50 µM PYR-41, right

Figure 6 | *continued.* panel) with Cy5-UbDha or -Ub electroporated into HeLa cells. Asterisks (*) indicate modified forms of E1 and E2 enzymes. c) Representative 3D confocal compilations compilations of fixed cells of fixed cells (from c) treated as indicated. Overlays of GFP (green) with Cy5-UbDha (magenta) along with corresponding pixel plots are shown; scale bars = 10 µm. d) Colocalization (Mander's overlap coefficient) of Cy5-UbDha with wild type (J1) or mutant (CS) GFP-UBE2J1 (n = 2, error bars correspond to SD, with significance (p) assessed using a two-sided t-test).

Discussion

Given the critical roles of E1, E2, and E3 enzymes in a wide range of biological processes and their resulting emergence as drug targets[41,42], there is a critical need for suitable assay reagents to study their function. The pyramidal structure of the Ub/Ubl conjugation systems, their complex cross-reactivities, and the reactive nature of the E2~Ub and E3~Ub thioester intermediates present practical challenges in dissecting interactions between Ub-loaded partner enzymes. To monitor these enzymatic cascades, we present a unique probe designed to hop from one active site to the next, leaving a detectable covalent mark at every step of the way.

Relatively inert on its own, our cascading probe (UbDha) requires ATP-dependent activation by the E1 enzyme, which increases the electrophilic character of the Dha moiety, making it suitable to follow the cascade of trans-thioesterification reactions downstream. The key conceptual advantage of Dha-based methodology lies in its unprecedented ability to choose at any point along the cascade between a native-like thioester and irreversible thioether bond formation. Indeed, we show that UbDha readily labels active site Cys residues of E1, E2, and HECT E3 enzymes.

Importantly, UbDha does not get transferred to substrates. This feature endows our cascade probe with advantageous capabilities over the native Ub, particularly in complex biological settings, where enzymes are present together with their substrates. Under such circumstances, UbDha enables a direct measure of enzyme activity, rather than merely detecting consequences thereof.

Because entry of Ub(/Ubl)Dha into its cognate enzymatic cascade requires ATP, much of the background binding to the probe can be easily discriminated by eliminating ATP with apyrase. This simple feature makes UbDha suitable for activity-based profiling of Ub/Ubl cascades not only in vitro, but also in complex biological circumstances, as demonstrated by the proteome-wide analysis of Ub conjugation machineries isolated from two different cancer cell lines. The straightforward nature of the experimental setup is expected to be readily adaptable to comparative profiling of E1, E2 (and to some degree E3 enzymes) as a function of various biological perturbations (i.e. stimulation or starvation, infection, etc.).

The same reagent can subsequently be used to study the effects of mutations in enzymes isolated directly from organisms of interest, as well as test for relevant factors upstream or downstream in the cascade. Standard biochemical techniques presently relied upon for such studies typically involve laborious expression and purification protocols. Furthermore, no observable reactivity in such preparations may be attributable to misfolding or lack of necessary modifications acquired in the carrier organism. Our methodology bypasses these difficulties by offering a relatively quick and easy way to assess reactivity of enzymes isolated directly from cells using simple immuno-precipitation. Then, taking cellular enzymology one step further, UbDha can be introduced into living cells to directly monitor enzymatic activities occurring in their natural context. In this way, the versatility of the UbDha cascade probe may prove invaluable in dissecting how aberrant activities of E1-E2-E3 cascades contribute to pathogenesis[45,46], as well as for diagnosis and monitoring efficacy of UPS targeting therapy. Furthermore, by generating a NEDD8-based counterpart of the UbDha probe capable of labeling the NEDD8 conjugating machinery, we show our method to be diversifiable towards Ubiquitin-like proteins. As such, the technology described here may be used to interrogate presently less well-defined ligation machineries of various Ubls.

In addition to cell-based applications, Ub/UblDha may prove useful in vitro, particularly for structure determination. The thioether adducts described here bypass the need for the often relied upon active site mutagenesis[13-17] thus avoiding potential disturbances to catalytic properties of enzymes in question. Stability of our thioether adducts under reducing conditions, in the presence of an activating E3 ligase and in functional assays allowed us to perform NMR and X-ray crystallography studies. High degree of similarity to the published oxyester-linked structure supports their utility as stable mimics in both structural and functional studies. We foresee that UbDha may be used to expedite generation of crystal structures of E1, E2, or E3 enzymes and their complexes[27]. In addition, we hypothesize that the stability of our E2-UbDha adducts immobilized on affinity beads could enable proteomic profiling of cognate RING E3 enzymes, which cannot themselves be directly trapped in a mechanism-dependent manner[43].

Based on the proof-of-concept studies described herein, we anticipate our cascading probe reagents to greatly facilitate future discoveries on Ub/Ubl conjugation.

Acknowledgements

We thank members of the Ovaa lab for helpful discussion and reagents, Dr. Jason Brown and Sian Armour (Ubiquigent) for providing the E2^{scan} kit and Dris El Atmioui for solid phase peptide synthesis. We acknowledge beam-line staff at Diamond I04-1 for expert help. Work was supported by a VICI grant from the Netherlands Organization for Scientific Research (N.W.O.) [724013002] to H.O., a Marie Curie ITN fellowship [290257] to K.W. and EMBO long term fellowships to I.B. and J.N.P. Work in the DK lab is funded by Medical Research Council [U105192732], the European Research Council [309756], and the Lister Institute for Preventive Medicine. Work in the BAS lab is funded by ALSAC, HHMI, and NIH grant R37GM069530. Work in the A.C.O.V. lab is funded by N.W.O [93511037] and the European Research Council [310913]. Work in the M.G. lab is funded by the German Research Foundation (DFG) CRC969 - project C01. J.B. received a stipend from the Graduate School Chemical Biology Ko-RSCB.

Author contributions

M.P.C.M. and F.E. designed the study. M.P.C.M., K.W. and I.B. carried out all labeling experiments. I.B. and K.W. designed and executed in-cell labeling experiments with assistance from R.M, and I.B. collected and analyzed confocal microscopy data. Mass spectrometry and relevant data analysis were performed by J.C. and A.C.O.V. on samples prepared by K.W. and I.B. J.N.P. and D.K. performed structural and competition studies and analyzed NMR and X-ray data. K.P.W. and B.A.S. generated the panel of purified HECT and NEDD8 pathway enzymes and helped with data analysis. J.B. and M.G. provided UBA6. M.P.C.M., F.E. and H.O. managed the study. M.P.C.M. and I.B. wrote the manuscript with input from other authors.

References

1. Komander, D. & Rape, M. The Ubiquitin code. Annu Rev Biochem 81, 203-29 (2012).
2. Steele-Mortimer, O. Exploitation of the Ubiquitin system by invading bacteria. Traffic 12, 162-9 (2011).
3. Sadaghiani, A.M., Verhelst, S.H. & Bogyo, M. Tagging and detection strategies for activity-based proteomics. Curr Opin Chem Biol 11, 20-8 (2007).
4. Cravatt, B.F., Wright, A.T. & Kozarich, J.W. Activity-based protein profiling: from enzyme chemistry to proteomic chemistry. Annu Rev Biochem 77, 383-414 (2008).
5. Borodovsky, A. et al. A novel active site-directed probe specific for deubiquitylating enzymes reveals proteasome association of USP14. EMBO J 20, 5187-96(2001).
6. Borodovsky, A. et al. Chemistry-based functional proteomics reveals novel members of the deUbiquitinating enzyme family. Chem Biol 9, 1149-59 (2002).
7. Ekkebus, R., Flierman, D., Geurink, P.P. & Ovaa, H. Catching a DUB in the act: novel Ubiquitin-based active site directed probes. Curr Opin Chem Biol 23, 63-70 (2014).
8. Kramer, H.B., Nicholson, B., Kessler, B.M. & Altun, M. Detection of Ubiquitin-proteasome enzymatic activities in cells: application of activity-based probes to inhibitor development. Biochim Biophys Acta 1823, 2029-37 (2012).
9. Lu, X. et al. Designed semisynthetic protein inhibitors of Ub/Ubl E1 activating enzymes. J Am Chem Soc 132, 1748-9 (2010).
10. Olsen, S.K., Capili, A.D., Lu, X., Tan, D.S. & Lima, C.D. Active site remodelling accompanies thioester bond formation in the SUMO E1. Nature 463, 906-12 (2010).
11. An, H. & Statsyuk, A.V. Development of activity-based probes for Ubiquitin and Ubiquitin-like protein signaling pathways. J Am Chem Soc 135, 16948-62 (2013).
12. An, H. & Statsyuk, A.V. Facile synthesis of covalent probes to capture enzymatic intermediates during E1 enzyme catalysis. Chem Commun 52, 2477-2480 (2016).
13. Wiener, R., Zhang, X., Wang, T. & Wolberger, C. The mechanism of OTUB1-mediated inhibition of Ubiquitination. Nature 483, 618-22 (2012).
14. Kamadurai, H.B. et al. Insights into Ubiquitin transfer cascades from a structure of a UbcH5B approximately Ubiquitin-HECT(NEDD4L) complex. Mol Cell 36, 1095-102 (2009).
15. Pruneda, J.N. et al. Structure of an E3:E2~Ub complex reveals an allosteric mechanism shared among RING/U-box ligases. Mol Cell 47, 933-42 (2012).
16. Scott, D.C. et al. Structure of a RING E3 trapped in action reveals ligation mechanism for the Ubiquitin-like protein NEDD8. Cell 157, 1671-84 (2014).
17. Plechanovova, A., Jaffray, E.G., Tatham, M.H., Naismith, J.H. & Hay, R.T. Structure of a RING E3 ligase and Ubiquitin-loaded E2 primed for catalysis. Nature 489, 115-20 (2012).
18. Schulman, B.A. & Harper, J.W. Ubiquitin-like protein activation by E1 enzymes: the apex for downstream signalling pathways. Nat Rev Mol Cell Biol 10, 319-31 (2009).
19. Hodgins, R.R., Ellison, K.S. & Ellison, M.J. Expression of a Ubiquitin derivative that conjugates to protein irreversibly produces phenotypes consistent with a Ubiquitin deficiency. J Biol Chem 267, 8807-12 (1992).
20. Pickart, C.M., Kasperek, E.M., Beal, R. & Kim, A. Substrate properties of site-specific mutant Ubiquitin protein (G76A) reveal unexpected mechanistic features of Ubiquitin-activating enzyme (E1). J Biol Chem 269, 7115-23 (1994).
21. Rotin, D. & Kumar, S. Physiological functions of the HECT family of Ubiquitin ligases. Nat Rev Mol Cell Biol 10, 398-409 (2009).
22. El Oualid, F. et al. Chemical synthesis of Ubiquitin, Ubiquitin-based probes, and diUbiquitin. Angew Chem Int Ed Engl 49, 10149-53 (2010).
23. Bernardes, G.J., Chalker, J.M., Errey, J.C. & Davis, B.G. Facile conversion of cysteine and alkyl cysteines to dehydroalanine on protein surfaces: versatile and switchable access to functionalized proteins. J Am Chem Soc 130, 5052-3 (2008).
24. Chalker, J.M. et al. Methods for converting cysteine to dehydroalanine Chem Sci 2, 1666-1676 (2011).
25. Jin, J., Li, X., Gygi, S.P. & Harper, J.W. Dual E1 activation systems for Ubiquitin differentially regulate E2 enzyme charging. Nature 447, 1135-8 (2007).
26. Schafer, A., Kuhn, M. & Schindelin, H. Structure of the Ubiquitin-activating enzyme loaded with two Ubiquitin molecules. Acta Crystallogr D Biol Crystallogr 70, 1311-20 (2014).
27. Olsen, S.K. & Lima, C.D. Structure of a Ubiquitin E1-E2 complex: insights to E1-E2 thioester transfer. Mol Cell 49, 884-96 (2013).
28. Andersen, P.L. et al. Distinct regulation of Ubc13 functions by the two Ubiquitin-conjugating enzyme variants Mms2 and Uev1A. J Cell Biol 170, 745-55 (2005).
29. Kee, Y., Lyon, N. & Huibregtse, J.M. The Rsp5 Ubiquitin ligase is coupled to and antagonized by the Ubp2 deUbiquitinating enzyme. EMBO J 24, 2414-24 (2005).
30. Ekkebus, R. et al. On terminal alkynes that can react with active-site cysteine nucleophiles in proteases. J Am Chem Soc 135, 2867-70 (2013).
31. Walden, H. et al. The structure of the APPBP1-UBA3-NEDD8-ATP complex reveals the basis for selective Ubiquitin-like protein activation by an E1. Mol Cell 12, 1427-37 (2003).
32. Pruneda, J.N., Stoll, K.E., Bolton, L.J., Brzovic, P.S. & Klevit, R.E. Ubiquitin in motion: structural studies of the Ubiquitin-conjugating enzyme approximately Ubiquitin conjugate. Biochemistry 50, 1624-33 (2011).
33. Page, R.C., Pruneda, J.N., Amick, J., Klevit, R.E. & Misra, S. Structural insights into the conformation and oligomerization of E2~Ubiquitin conjugates. Biochemistry 51, 4175-87 (2012).
34. van Wijk, S.J. & Timmers, H.T. The family of Ubiquitin-conjugating enzymes (E2s): deciding between life and death of proteins. FASEB J 24, 981-93 (2010).
35. Huang, L. et al. Structure of an E6AP-UbcH7 complex: insights into Ubiquitination by the E2-E3 enzyme cascade. Science 286, 1321-6 (1999).
36. Nakada, S. et al. Non-canonical inhibition of DNA damage-dependent Ubiquitination by OTUB1. Nature 466, 941-6 (2010).
37. Yang, Y. et al. Inhibitors of Ubiquitin-activating enzyme (E1), a new class of potential cancer therapeutics. Cancer Res 67, 9472-81 (2007).
38. Dantuma, N.P., Groothuis, T.A., Salomons, F.A. & Neefjes, J. A dynamic Ubiquitin equilibrium couples proteasomal activity to chromatin remodeling. J Cell Biol 173, 19-26 (2006).
39. Pohl, C. & Jentsch, S. Final stages of cytokinesis and midbody ring formation are controlled by BRUCE. Cell 132, 832-45 (2008).

40. Menon, M.B. et al. Endoplasmic reticulum-associated Ubiquitin-conjugating enzyme Ube2j1 is a novel substrate of MK2 (MAPKAP kinase-2) involved in MK2-mediated TNFalpha production. Biochem J 456, 163-72 (2013).
41. Liu, J. et al. Targeting the Ubiquitin pathway for cancer treatment. Biochim Biophys Acta 1855, 50-60 (2015).
42. da Silva, S.R., Paiva, S.L., Lukkarila, J.L. & Gunning, P.T. Exploring a new frontier in cancer treatment: targeting the Ubiquitin and Ubiquitin-like activating enzymes. J Med Chem 56, 2165-77 (2013).
43. Sommer, S., Ritterhoff, T., Melchior, F. & Mootz, H.D. A stable chemical SUMO1-Ubc9 conjugate specifically binds as a thioester mimic to the RanBP2-E3 ligase complex. Chembiochem 16, 1183-9 (2015).

25. Jin, J., Li, X., Gygi, S.P. & Harper, J.W. Dual E1 activation systems for Ubiquitin differentially regulate E2 enzyme charging. Nature 447, 1135-8 (2007).
26. Schafer, A., Kuhn, M. & Schindelin, H. Structure of the Ubiquitin-activating enzyme loaded with two Ubiquitin molecules. Acta Crystallogr D Biol Crystallogr 70, 1311-20 (2014).
27. Olsen, S.K. & Lima, C.D. Structure of a Ubiquitin E1-E2 complex: insights to E1-E2 thioester transfer. Mol Cell 49, 884-96 (2013).
28. Andersen, P.L. et al. Distinct regulation of Ubc13 functions by the two Ubiquitin-conjugating enzyme variants Mms2 and Uev1A. J Cell Biol 170, 745-55 (2005).
29. Kee, Y., Lyon, N. & Huibregtse, J.M. The Rsp5 Ubiquitin ligase is coupled to and antagonized by the Ubp2 deUbiquitinating enzyme. EMBO J 24, 2414-24 (2005).
30. Ekkebus, R. et al. On terminal alkynes that can react with active-site cysteine nucleophiles in proteases. J Am Chem Soc 135, 2867-70 (2013).
31. Walden, H. et al. The structure of the APPBP1-UBA3-NEDD8-ATP complex reveals the basis for selective Ubiquitin-like protein activation by an E1. Mol Cell 12, 1427-37 (2003).
32. Pruneda, J.N., Stoll, K.E., Bolton, L.J., Brzovic, P.S. & Klevit, R.E. Ubiquitin in motion: structural studies of the Ubiquitin-conjugating enzyme approximately Ubiquitin conjugate. Biochemistry 50, 1624-33 (2011).
33. Page, R.C., Pruneda, J.N., Amick, J., Klevit, R.E. & Misra, S. Structural insights into the conformation and oligomerization of E2~Ubiquitin conjugates. Biochemistry 51, 4175-87 (2012).
34. van Wijk, S.J. & Timmers, H.T. The family of Ubiquitin-conjugating enzymes (E2s): deciding between life and death of proteins. FASEB J 24, 981-93 (2010).
35. Huang, L. et al. Structure of an E6AP-UbcH7 complex: insights into Ubiquitination by the E2-E3 enzyme cascade. Science 286, 1321-6 (1999).
36. Nakada, S. et al. Non-canonical inhibition of DNA damage-dependent Ubiquitination by OTUB1. Nature 466, 941-6 (2010).
37. Yang, Y. et al. Inhibitors of Ubiquitin-activating enzyme (E1), a new class of potential cancer therapeutics. Cancer Res 67, 9472-81 (2007).
38. Dantuma, N.P., Groothuis, T.A., Salomons, F.A. & Neefjes, J. A dynamic Ubiquitin equilibrium couples proteasomal activity to chromatin remodeling. J Cell Biol 173, 19-26 (2006).
39. Pohl, C. & Jentsch, S. Final stages of cytokinesis and midbody ring formation are controlled by BRUCE. Cell 132, 832-45 (2008).
40. Menon, M.B. et al. Endoplasmic reticulum-associated Ubiquitin-conjugating enzyme Ube2j1 is a novel substrate of MK2 (MAPKAP kinase-2) involved in MK2-mediated TNFalpha production. Biochem J 456, 163-72 (2013).
41. Liu, J. et al. Targeting the Ubiquitin pathway for cancer treatment. Biochim Biophys Acta 1855, 50-60 (2015).
42. da Silva, S.R., Paiva, S.L., Lukkarila, J.L. & Gunning, P.T. Exploring a new frontier in cancer treatment: targeting the Ubiquitin and Ubiquitin-like activating enzymes. J Med Chem 56, 2165-77 (2013).
43. Sommer, S., Ritterhoff, T., Melchior, F.& Mootz, H.D. A stable chemical SUMO1-Ubc9 conjugate specifically binds as a thioester mimic to the RanBP2-E3 ligase complex. Chembiochem 16, 1183-9 (2015).

Supplementary Information

SYNTHETIC PROCEDURES

General Fmoc SPPS Strategy. The Ub (mutant) peptide sequences were synthesized on resin following the procedures described before.[1,2]

Synthesis Ub-Dha. Method A: 50 µmol Fmoc-Ub(1-75)-OH was dissolved in 15 mL DCM and treated overnight with 5 eq pyBOP (0.25 mmol, 130 mg), 10 eq DiPEA (0.5 mmol, 87 µL) and 5 eq H-Cys(Bn)-OMe (HCl salt) (0.25 mmol, 65 mg). The organic layer was washed with 1M KHSO4, dried with Na2SO4 and concentrated. The crude product was dissolved in 20 mL DCM and treated overnight with 5 eq DBU (37 µL) followed by another 2 hrs with fresh DBU (5 eq, 37 µL). The organic layer was washed with 1M KHSO4, dried with Na2SO4 and concentrated. Next, the product was totally deprotected by treatment for 3 hrs in 10 mL of TFA/H2O/iPr3SiH/PhOH (90/5/2.5/2.5; v/v/v/v). The crude product was precipitated in 90 mL cold diethyl ether/n-pentane 3/1 v/v and pelleted at 1500 rpm for 10 min; this was repeated 3× using diethyl ether to wash the precipitated product. The product was dissolved in 5 mL DMSO and diluted into 20 mL milliQ containing 5% acetonitrile and 0.05% TFA (buffer A HPLC). The obtained mixture was purified by RP-HPLC using 2 mobile phases: A=0.05% TFA and 5% acetonitrile in milliQ and B: 0.05% TFA and 5% milliQ in CH3CN. Waters C18 XBridge 5 µM, 130Å (30×150 mm); flowrate: 30 mL/min. Gradient: 25à75% B over 15 min. Pure fractions were pooled and lyophilized. Yield UbGly76Cys(Bn)-OMe: 135 mg, 15.5 µmol, 31%. ES MS+ (amu) calcd: 8715, found 8714. Next, 65 mg (7.5 µmol) UbGly76Cys(Bn)-OMe was dissolved in 1 mL DMSO and diluted into 40 mL 50 mM sodium phosphate pH 8. A solution of MSH (10 eq, 16 mg) in 1 mL DMF was added to the reaction mixture and after stirring for 2 hrs, LC-MS analysis showed complete elimination of the Cys(Bn) into the Dha moiety. The reaction had turn cloudy and centrifugation (30 min, 4000 rpm) allowed removal of any precipitated material; LC-MS analysis of this precipitate (dissolved in DMSO) showed that this was not the product. The clear solution containing the product was brought to pH 10 with 10N NaOH. After 90 min, LC-MS analysis showed complete hydrolysis of the methyl ester. RP-HPLC purification as described above, gave the desired Ub-Dha (66.5 mg; 7.8 µmol) in 50 % yield. ES MS+ (amu) calcd: 8577, found 8577.

Synthesis Ub-Dha. Method B: The C-terminal glycine in Ub was mutated to a cysteine by site directed mutagenesis. Next, Ub G76C was expressed in autoinduction3 media at 37°C using E. coli BL21 (DE3). After 2-3 hours the temperature was lowered to 18°C and the bacteria were allowed to grow an additional 12h. Cells were harvested by centrifugation (4000 rpm, 4°C), resuspended in lysis buffer, lysed by sonication on ice, and centrifuged for 30 min at 20 000 g at 4°C to remove all cell debris. The soluble lysate was then treated

with 2.5 mM beta-mercaptoethanol for 10 min before being heated to 85°C to precipitate contaminating proteins which were removed by centrifugation (20 000 rpm, 20 min 4°C). The pH of the cleared lysate (about 90% purity) was adjusted to pH 4.7 using 1M NH4OAc before being loaded onto a cation exchange column (40S Workbeads, BioWorks). Next, the peptide was purified using a MonoS column and 0–1 M NaCl gradient in 50 mM NaOAc pH 4.5. Fractions with product were pooled and further purified by prep-HPLC using 2 mobile phases: A=0.05% TFA in milliQ and B: 0.05% TFA in CH3CN. Prep-HPLC program: Waters C18 XBridge 5 µM, 130Å (30×150 mm); flowrate: 30 mL/min. Gradient: 0 – 6 min: 5 à 25% B; 6 - 21 min: 25 à 75% B; 21 – 23 min: 75 à 95% B. The purified UbG76C was lyophilized and used as a precursor for the elimination reaction with the dibromide.

UbG76C (215 mg; 25.0 µmol) was dissolved in 2 mL of DMSO and added slowly to MilliQ (75 mL). This was diluted with 100 mM sodium phosphate pH8.0 to a final volume of 150 mL (50 mM NaP pH 8). Next, 2,5-dibromohexandiamide (75.4 mg; 250 µmol) was added. The reaction mixture was incubated at 37ºC overnight and spun down to remove the insoluble dibromide. RP-HPLC purification as described above, gave the desired Ub-Dha (96 mg, 11.2 umol, 45%). ES MS+ (amu) calcd: 8577, found 8577.

Synthesis Cy5-Ub-Dha. 80 µmol Cy5-Ub(1-75)-OH was dissolved in 20 mL DCM and treated overnight with 5 eq pyBOP (400 µmol, 208 mg), 10 eq DiPEA (800 µmol, 144 µL) and 5 eq H-Cys(Bn)-OMe (HCl salt) (400 µmol, 104 mg). The organic layer was washed with 1M KHSO4, dried with Na2SO4 and concentrated. Next, the product was totally deprotected by treatment for 3 hrs in 15 mL of TFA/H2O/iPr3SiH/PhOH (90/5/2.5/2.5; v/v/v/v). The crude product was precipitated in 150 mL cold diethyl ether/n-pentane 3/1 v/v and pelleted at 1500 rpm for 10 min; this was repeated 3× using diethyl ether to wash the precipitated product. The product was dissolved in 10 mL DMSO and diluted into 50 mL milliQ containing 5% acetonitrile and 0.05% TFA (buffer A HPLC). The obtained mixture was purified by RP-HPLC as described for Ub-Dha. Yield Cy5-UbGly76Cys(Bn)-OMe: 190 mg, 20 µmol, 26%. ES MS+ (amu) calcd: 9194, found 9194. Next, 60 mg (6.5 µmol) Cy5- UbGly76Cys(Bn)-OMe was dissolved in 1 mL DMSO and diluted into 40 mL milliQ. Next, this solution was buffered to 50 mM sodium phosphate with a 0.4M sodium phosphate stock of pH 6.8; the pH was adjusted with 10N NaOH to pH 8. A solution of MSH (10 eq, 65 µmol, 14 mg) in 0.5 mL DMF was added to the reaction mixture and after stirring for 2 hrs, LC-MS analysis showed complete transformation of the Cys(Bn) group into a Dha moiety. The reaction had turned cloudy and centrifugation (30 min, 4000 rpm) allowed removal of precipitated material; LC-MS analysis of this precipitate (dissolved in DMSO) showed that this contained no product. The clear solution with the product was brought to pH 10 with 10N NaOH. After 90 min, LC-MS analysis showed complete hydrolysis of the methyl ester. RP-HPLC purification as described above, gave the desired Cy5- Ub-Dha (25 mg; 2.8 µmol) in 40 % yield. ES MS+ (amu) calcd: 9069, found 9070.

Synthesis Biotin-PEG-Ub-Dha. 20 µmol Biotin-PEG-Ub(1-75)-OH was dissolved in 5 mL DCM and treated overnight with 5 eq pyBOP (0.1 mmol, 52 mg), 10 eq DiPEA (0.2 mmol, 36 µL) and 5 eq H-Cys(Bn)-OMe (HCl salt) (0.1 mmol, 26 mg). The organic layer was washed with 1M KHSO4, dried with Na2SO4 and concentrated. Next, the product was totally deprotected by treatment for 3 hrs in 2 mL of TFA/H2O/iPr3SiH/PhOH (90/5/2.5/2.5; v/v/v/v). The crude product was precipitated in cold diethyl ether/n-pentane 3/1 v/v and pelleted at 1500 rpm for 10 min; this was repeated 3× using diethyl ether to wash the precipitated product. The product was dissolved in 2 mL DMSO and diluted into 15 mL milliQ containing 5% acetonitrile and 0.05% TFA (buffer A HPLC). The obtained mixture was purified by RP-HPLC as described for Ub-Dha. Yield Biotin-PEG-UbGly76Cys(Bn)-OMe: 17 mg, 1.9 µmol, 10%. ES MS+ (amu) calcd: 9086, found 9085. Next, 4.8 mg (0.53 µmol) Biotin-PEG-UbGly76Cys(Bn)-OMe was dissolved in 0.4 mL DMSO and diluted into 10 mL 50 mM sodium phosphate pH 8. A solution of MSH (10 eq, 1.2 mg) in 100 µL DMF was added to the reaction mixture and after stirring for 2 hrs, LC-MS analysis showed complete transformation of the Cys(Bn) group into a Dha moiety. The reaction had turn cloudy and centrifugation (30 min, 4000 rpm) allowed removal of precipitated material; LC-MS analysis of this precipitate (dissolved in DMSO) showed that this contained no product. The clear solution with the product was brought to pH 10 with 10N NaOH. After 90 min, LC-MS analysis showed complete hydrolysis of the methyl ester. RP-HPLC purification as described above, gave the desired Biotin-PEG- Ub-Dha (2.5 mg; 0.29 µmol) in 55% yield. ES MS+ (amu) calcd: 8948, found 8948.

SynthesisNEDD8Dhafromsynthetic NEDD8G76CSPPSofNEDD8G76Cwasperformedona Syro II MultiSyntech Automated Peptide synthesizer using standard 9-fluorenylmethoxycarbonyl (Fmoc) based solid phase peptide chemistry at 100 µmol scale, a 4-fold excess of amino acids and pyBOP and a 8-fold excess of DiPEA relative to Fmoc-L-Cys(Trt)-PEG-PS (0.20 mmol/g, Applied Biosystems®) resin. All amino acids were double coupled except for the dipeptide building blocks. Dipeptides Fmoc-L-Leu-L-Thr(ΨMe,Mepro)-OH, Fmoc-L-Tyr-L-Ser(ΨMe,Mepro)-OH and Fmoc-L-Gly-L-Ser(ΨMe,Mepro)-OH were single coupled for 1 hour. Fmoc removal was performed with 20% piperidine/NMP for 2 x 3 min and 1 x 8 min. Position of dipeptides used during SPPS of NEDD8 are shown below:

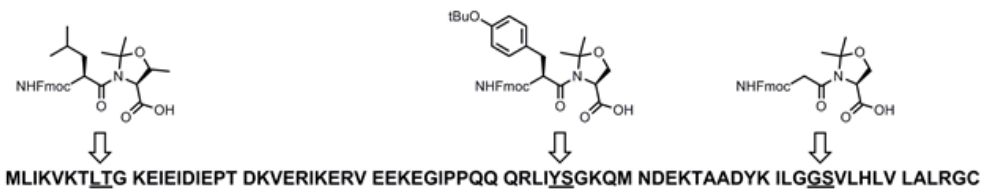

Next, the resin bound NEDD8 G76C was treated with TFA/H2O/iPr3SiH/PhOH (90/5/2.5/2.5; v/v/v/v) for 3 h. The crude product was precipitated in cold diethyl ether/n-pentane 3/1 v/v and pelleted at 1500 rpm for 10 min; this was repeated 3× using diethyl ether to wash the precipitated product. The pellet was dissolved in a mixture of H2O/CH3CN/HOAc (65/25/10 v/v/v) and finally lyophilized. The product was dissolved in 2 mL DMSO and diluted into 15 mL milliQ containing 5% acetonitrile and 0.05% TFA (buffer A HPLC). The obtained mixture was purified by RP-HPLC as described for Ub-Dha. ES MS+ (amu) calcd: 8606, found 8604. The pure fractions were combined, ACN was concentrated in vacuo and the remaining solution was diluted to a final volume of 100 mL in 50 mM sodium phosphate pH 8. Next, 2,5-dibromohexandiamide (500 mg, 1.66 mmol) was added and the reaction mixture incubated overnight at 37ºC overnight. Precipitated material derived from the dibromide was removed and RP-HPLC purification as described above, followed by SE purification gave the desired NEDD8-Dha (8 mg, 0.9 µmol, 1%). ES MS+ (amu) calcd: 8572, found 8572.

References

1. El Oualid, F. et al. Chemical synthesis of Ubiquitin, Ubiquitin-based probes, and diUbiquitin. Angew Chem Int Ed Engl 49, 10149-10153 (2010).
2. Mulder, M.P.C., El Oualid, F., ter Beek, J. & Ovaa, H. A native chemical ligation handle that enables the synthesis of advanced activity-based probes: diUbiquitin as a case study. Chembiochem 15, 946-949 (2014).
3. Studier, F.W. Protein production by auto-induction in high density shaking cultures. Protein Expr Purif 41, 207-234 (2005).

CHARACTERIZATION DATA

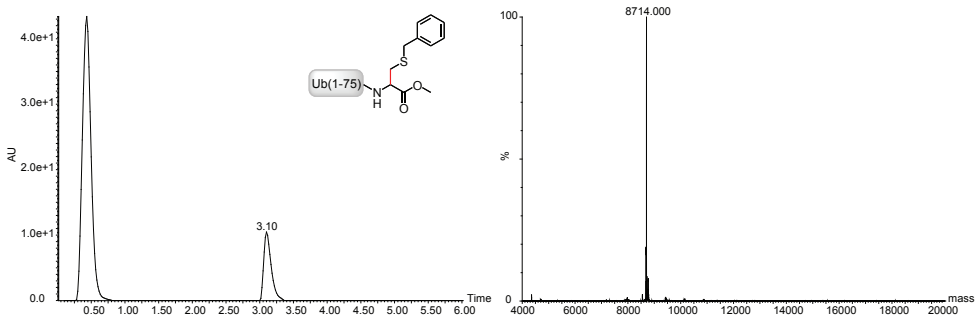

Figure 1. UbGly76Cys(Bn)OMe. Diode Array chromatogram (left). Deconvulated mass of product peak (right). ESI-Mass [M+H] Expected: 8715, Found: 8714.

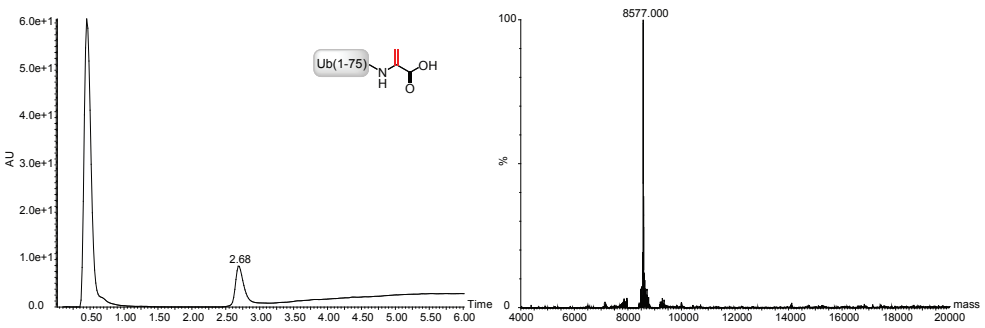

Figure 2. UbDha. Diode Array chromatogram (left). Deconvulated mass of product peak (right). ESI-Mass [M+H] Expected: 8577, Found: 8577

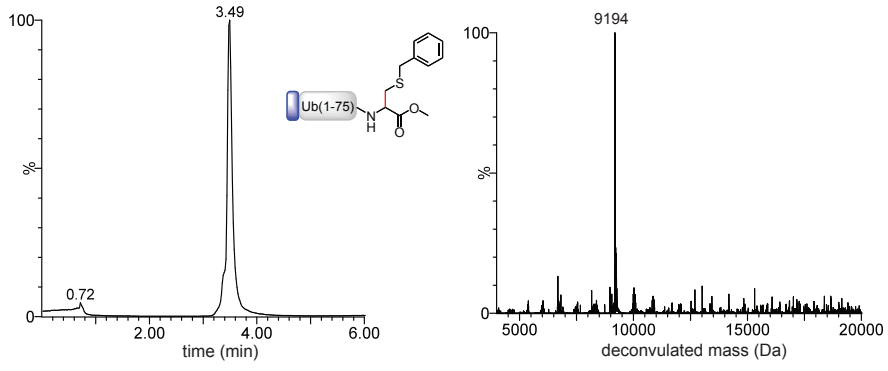

Figure 3. Cy5-Gly76Cys(Bn)OMe. Diode Array chromatogram (left). Deconvulated mass of product peak (right). ESI-Mass [M+H] Expected: 9194, Found: 9194

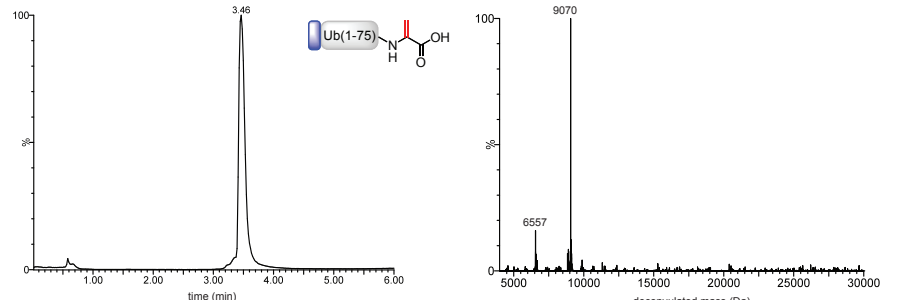

Figure 4. Cy5-UbDha. Diode Array chromatogram (left). Deconvulated mass of product peak (right). ESI-Mass [M+H] Expected: 9069, Found: 9070

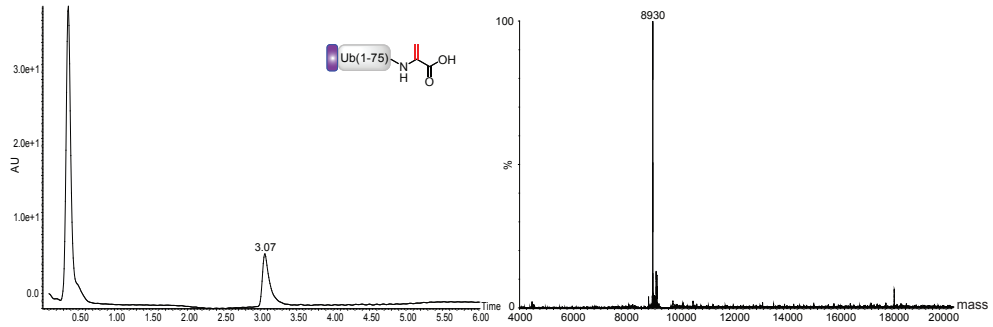

Figure 5. Rho-UbDha. Diode Array chromatogram (left). Deconvulated mass of product peak (right). ESI-Mass [M+H] Expected: 8930, Found: 8930

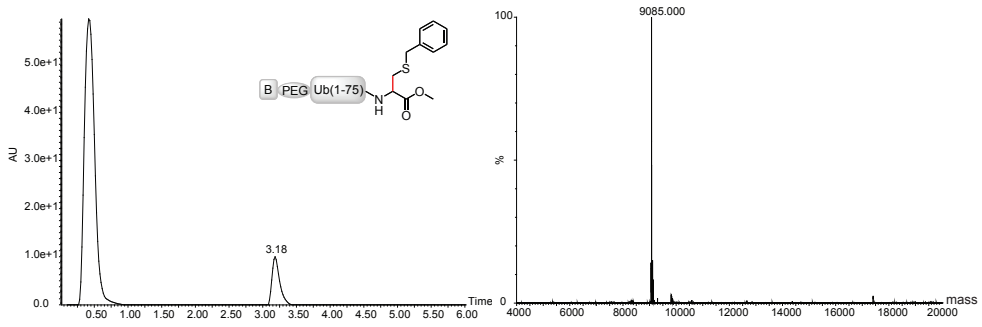

Figure 6. Biotin-PEG-Gly76Cys(Bn)OMe. Diode Array chromatogram (left). Deconvulated mass of product peak (right). ESI-Mass [M+H] Expected: 9086, Found: 9085

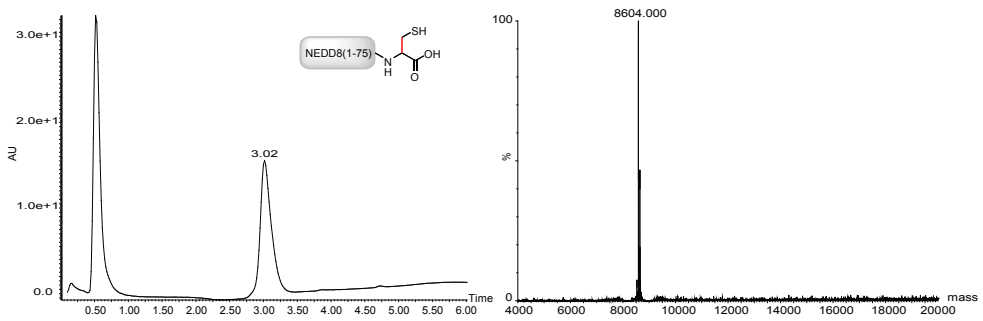

Figure 7. Biotin-PEG-UbDha. Diode Array chromatogram (left). Deconvulated mass of product peak (right). ESI-Mass [M+H] Expected: 8948, Found: 8948

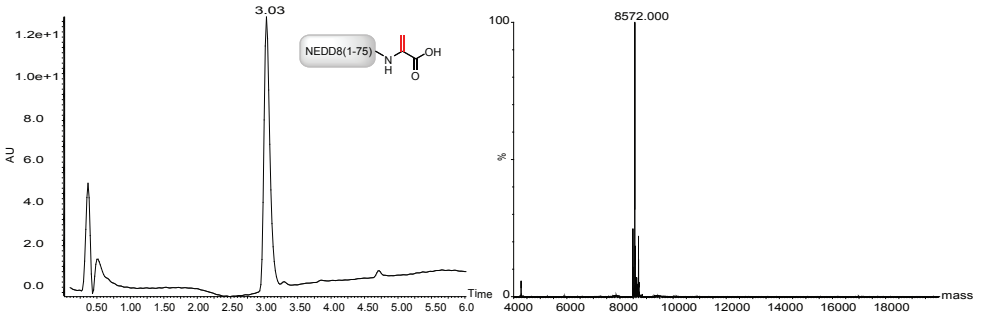

Figure 8. NEDD8 Gly76Cys. Diode Array chromatogram (left). Deconvulated mass of product peak (right). ESI-Mass [M+H] Expected: 8606, Found: 8604

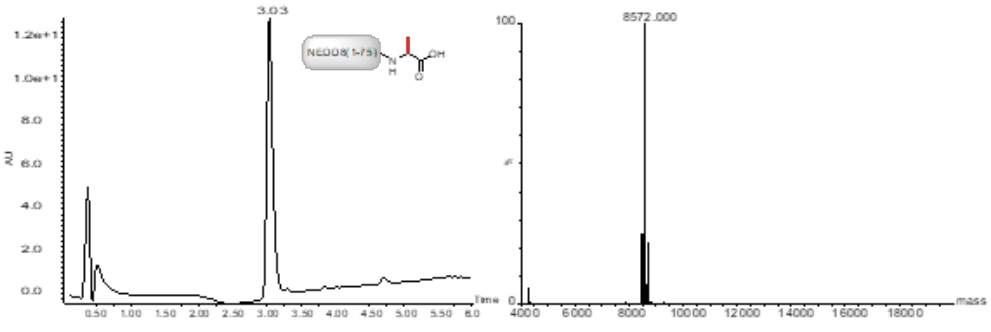

Figure 9. NEDD8Dha. Diode Array chromatogram (left). Deconvulated mass of product peak (right). ESI-Mass [M+H] Expected: 8572, Found: 8572

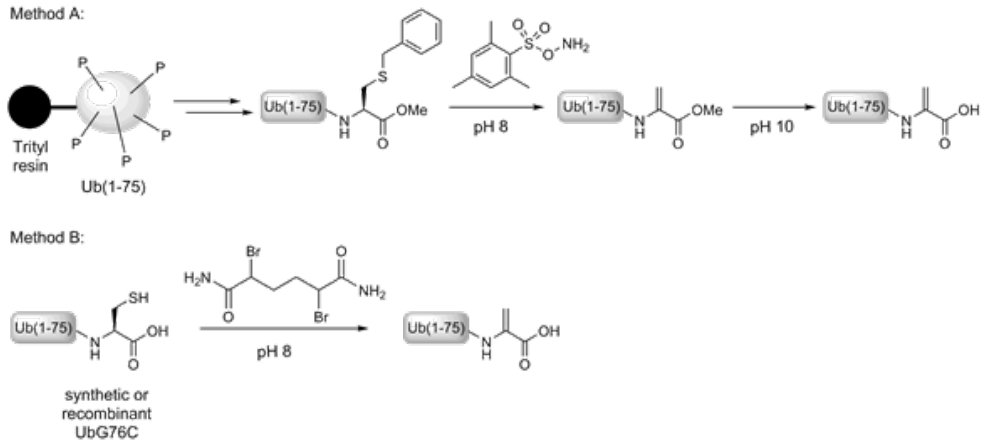

Supplementary Figure 1. Synthesis of Ub-Dha starting from Ub(1-75)-Cys(Bn)-OMe (method A) or UbG76C (method B).

E1-E2-E3 LABELLING ASSAY CONDITIONS

E1 labeling UBE1 or UBA6 (1 µM) in 50 mM HEPES pH 8, 100 mM NaCl, 10 mM $MgCl_2$ and 10 mM ATP was incubated with Ub-Dha probe (30 µM) at 37°C for 30 min. The reaction was quenched by the addition of reducing sample buffer and heating (90°C for 10 min). Samples were analyzed by SDS-PAGE and stained with Coomassie for analysis.

E2 labeling E2 enzyme (2.5 µM) and UBE1 (0.63 µM) in 50 mM HEPES pH 7.5, 100 mM NaCl, 5 mM $MgCl_2$ and 2 mM ATP was incubated with Ub-Dha probe (12.5 µM) at 37°C for 30 min. The reaction was quenched by the addition of reducing sample buffer and heating (90°C for 10 min). Samples were analyzed by SDS-PAGE and visualized by silver staining.

UBE2L3 E2 labeling – Comparison of UbDha and Ub UBE2L3 (2.5 µM) and UBE1 (0.3 or 1.25 µM) were incubated with Ub-Dha probe (25 µM) or Ub (25 µM) in 50 mM HEPES, 100 mM NaCl (pH 7.5), 5 mM $MgCl_2$ and 2 mM ATP at 37°C for 30 min. The reaction was quenched by the addition of reducing or non-reducing sample buffer. The samples with reducing sample buffer were heated (90°C for 10 min). Samples were analyzed by SDS-PAGE and visualized by silver staining.

pH effect on labeling Using the optimized protocols for E1 and E2 labeling, the effect of pH on labeling efficiency was evaluated using 50 mM HEPES pH 6.5, 7.0, 7.5, 8.0 or 8.5, 100 mM NaCl, 10 mM $MgCl_2$, and 5 mM ATP at 30°C for 60 min. In addition a no ATP control was taken along for pH 7.5. The reaction was quenched by the addition of reducing sample

buffer and heating (90°C for 10 min). Samples were analyzed by SDS-PAGE and visualized by fluorescence scanning (λex= 625 nm; λem= 680 nm) and silver stain.

E2 labeling assay–E2^{scan} Kit Panel (Ubiquigent) The E2^{scan} plate (cat. nr. 67-0005-001, Ubiquigent, Dundee, UK) was thawed on ice prior to use. The plate contains a panel of 34 E2 enzymes in duplicate. The duplicate E2 positions were used for non-ATP control experiments. Final ratios: E1/E2/probe = 0.63/2.5/12.5 µM in 50 mM HEPES pH 7.5, 5 mM $MgCl_2$ and 2.5 mM DTT. To 10 µl of E2 in the plate (5 µM), 5 µl of E1/probe mix (2.5 µM/ 50 µM) was added, followed by 5 µl of 8 mM ATP or 5 ul buffer (no ATP control). The plate was incubated for 2 hrs at 300C and reactions were quenched by the addition of sample buffer with beta-mercaptoethanol and heating (900C, 10 min). Samples were analyzed by SDS-PAGE and visualized by silver staining. *Note: the Ubiquitin loading activity of the enzymes with native Ub ranges from 0 - 70% (see leaflet E2 ^{scan} Kit Panel).*

HECT E3 labeling NEDD4L (2.5 µM) and UBE2D (0.5 µM) UBE1 (0.25 µM) were incubated with Cy5-Ub-Dha probe (50 µM) in 50 mM HEPES pH 7.5, 100 mM NaCl, 5 mM $MgCl_2$ and 2 mM ATP at 30°C for 2h. The reaction was quenched by the addition of reducing sample buffer and heating (90°C for 10 min). Samples were analyzed by SDS-PAGE and visualized by fluorescence scanning (λex= 625 nm; λem= 680 nm).

E3 panel Nine HECT E3 enzymes (HECT domain of human NEDD4, NEDD4L, ITCH, UBE3C, WWP1, WWP2, HACE1, WW3 + HECT domain of Smurf2 (human) and Rsp5 (*S. cerevisiae*); 2.5 µM) were incubated with UBE2D (0.5 µM) UBE1 (0.25 µM) and Ub-Dha probe (50 µM) in 50 mM HEPES pH 7.0, 100 mM NaCl, 5 mM $MgCl_2$ and 2 mM ATP at 30°C for 1h. Samples were resolved by SDS-PAGE and visualized by silver stain or western blot (Mouse Ub antibody: 1:1000 dilution; Santa Cruz, Ub(P4D1), sc-8017). E3 controls The HECT domains of Nedd4L wt, the Cys-to-Ala mutant, single cysteine (catalytic cysteine only) mutant and HECT domain of Smurf2 wt and Cys-to-Ala mutant (2.5 µM) were incubated with Ub-Dha probe (50 µM) in or without the presence of UBE2D (0.5 µM), UBE1 (0.25 µM) and 5 mM $MgCl_2$ and 2 mM ATP in 50 mM HEPES pH 7.0, 100 mM NaCl, at 30°C for 1h. Samples were resolved by SDS-PAGE and visualized by silver stain or western blot (Mouse Ub antibody: 1:1000 dilution; Santa Cruz, Ub(P4D1), sc-8017).

Turnover Ubiquitination of WBP2 WBP2 (crosslinked with Fluorescein; 0.2 µM) was incubated with HECT E3 enzyme (ΔC2 version of NEDD4L, Rsp5, WWP1 or WWP2; 1.5 µM), UBE2D (0.5 µM) UBE1 (50 nM) and UbDha probe or wt Ub (15 µM) in 50 mM HEPES pH 7.5, 100 mM NaCl, 10 mM $MgCl_2$ and 5 mM ATP at RT for 11 or 60 min. The reaction was quenched by the addition of reducing sample buffer and heating (90°C for 10 min). Samples were analyzed by SDS-PAGE and visualized by fluorescence scanning (λex= 473 nm; λem= 530 nm).

NEDD8Dha Labeling UBA3/NAE1 (2 µM) was incubated with NEDD8Dha probe (40 µM) or NEDD8 (40 µM) in 50 mM Tris pH 7.5, 300 mM NaCl, 10 mM $MgCl_2$ and 5 mM ATP at 30°C for 60 min. The reaction was quenched by the addition of reducing or non-reducing sample buffer. The samples with reducing sample buffer were heated (90°C for 10 min). Samples were analyzed by SDS-PAGE and visualized by silver stain.
UBE2M wt (2 µM) was incubated with UBA3/NAE1 (0.5 µM) and NEDD8Dha probe (20 µM) in buffer containing 50 mM Tris pH 7.5, 300 mM NaCl, 10 mM $MgCl_2$ and 5 mM ATP at 30°C for 60 min. The reaction was quenched by the addition of reducing sample buffer and heating (90°C for 10 min). Samples were analyzed by SDS-PAGE and visualized by silver stain.

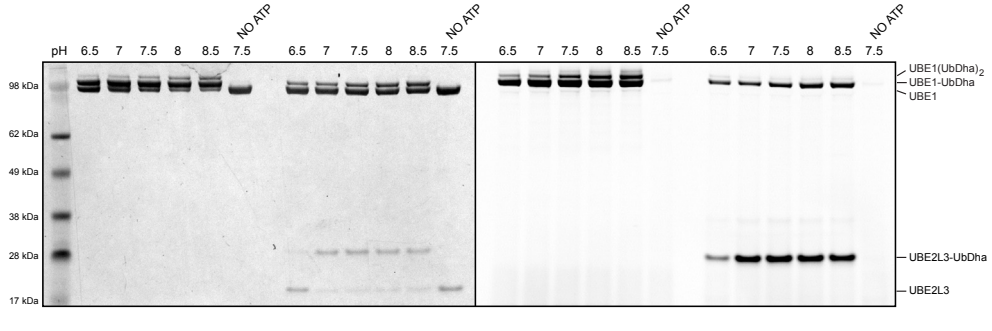

Supplementary Figure 2. pH effect on labeling of Cy5-UbDha with UBE1 and UBE2L3. Left: silver stain, right: fluorescent scan.

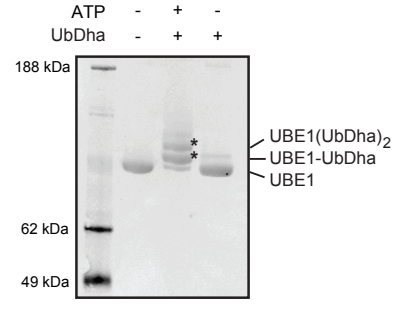

Supplementary Figure 3. Western Blot of UBE1 labeling reaction with UbDha (blotted against His-tagged UBE1) showing the UBE1-UbDha and UBE1(UbDha)2 adducts (indicated by asterisks).

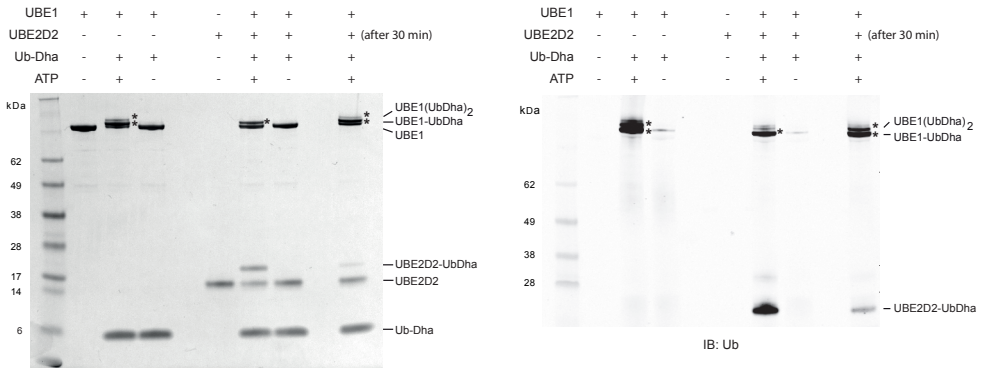

Supplementary Figure 4. Doubly loaded UBE1 intermediate is not formed in the presence of UBE2D2. Silver stain (left) and western blot against Ub (right). The asterisks indicate the thioether-linked UBE1-UbDha and UBE1(UbDha)2 adducts.

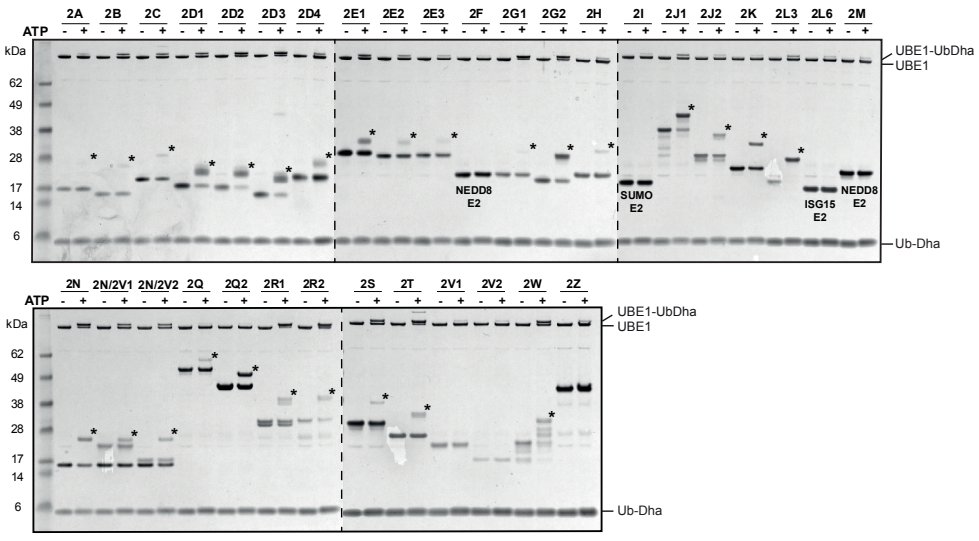

Supplementary Figure 5. UbDha labels 27 E2s specific for Ub transfer but not E2s employing Ubls. The asterisks indicate the thioether-linked E2-UbDha adducts. (E2-scan kit, Ubiquigent).Visualized by silver stain.

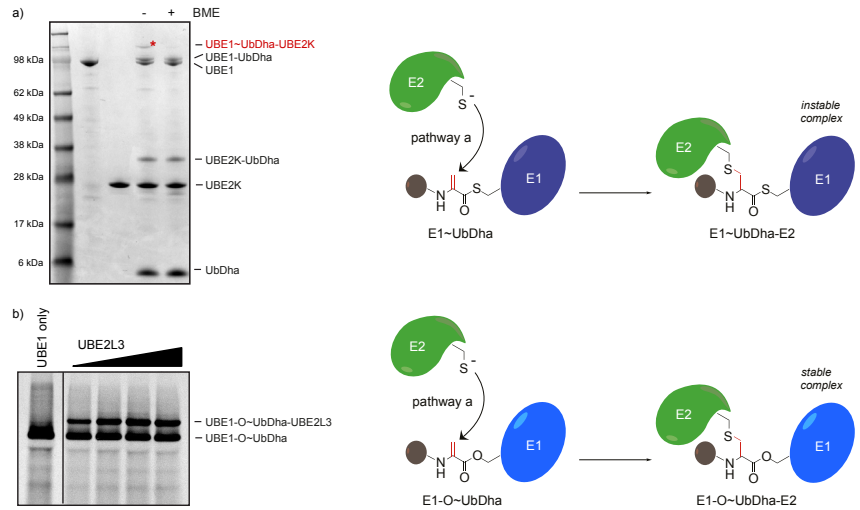

Supplementary Figure 6. A ternary complex is formed via a third pathway. The acceptor enzyme directly reacts with the Michael acceptor on the probe donating enzyme thioester adduct. a) SDS-PAGE analysis of UbDha reaction with UBE1 and UBE2K. Under non-reducing conditions the ternary complex is visible on gel, while under reducing conditions this instable complex is not (visualized by coomassie). b) In gel fluorescence analysis of Cy5-UbDha reaction with UBE1 active site Cys-Ser mutant and UBE2L3. Under reducing conditions the more stable ternary UBE1-O~UbDha-UBE2L3 is still visible.

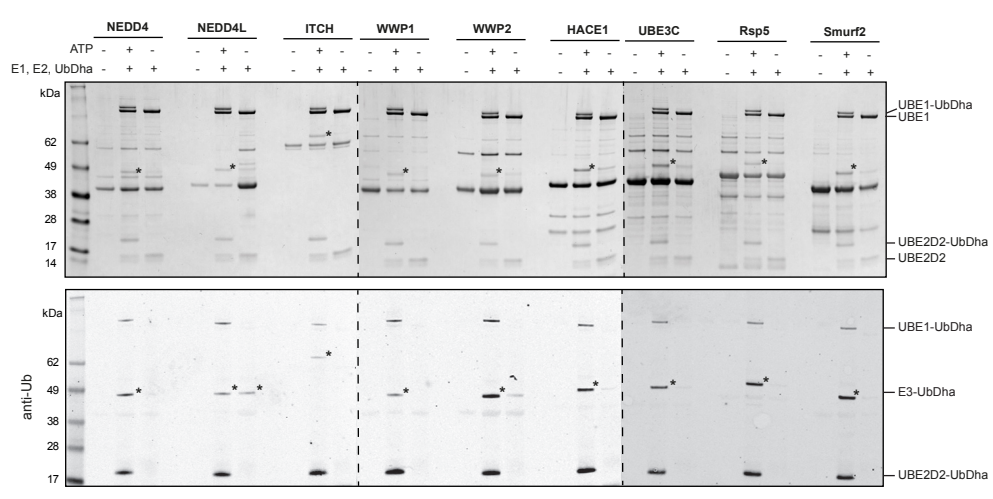

Supplementary Figure 7. UbDha shows reactivity towards E3 HECT enzymes under ATP dependent conditions. The asterisks indicate the E3-UbDha thioether-linked adduct. Visualized by silver staining (upper panel) and western blot against Ub (lower panel).

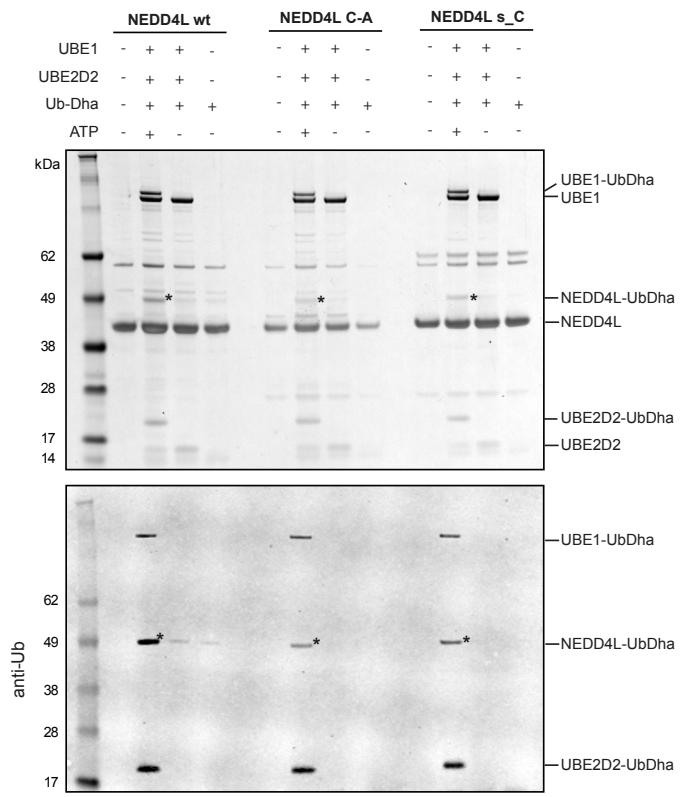

Supplementary Figure 8. Labeling of NEDD4L wt, Cys-to-Ala mutant and single Cys mutant with UbDha visualized by silver staining (upper panel) and western blot against Ub (lower panel). The asterisks indicate the thioether-linked NEDD4L-UbDha adduct.

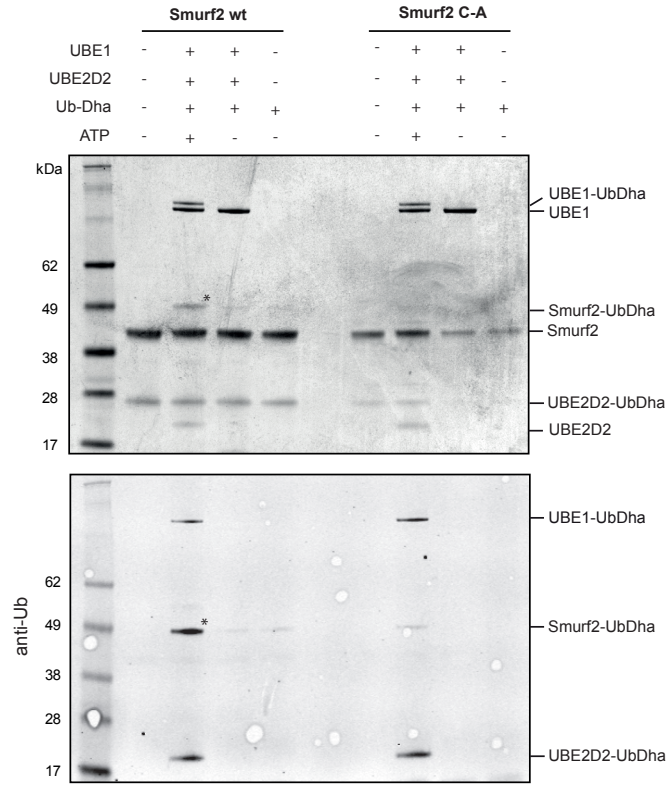

Supplementary Figure 9. Labeling of Smurf2 wt and Cys-to-Ala mutant with UbDha, visualized by silver staining (upper panel) and western blot against Ub (lower panel). The asterisks indicate the thioether-linked Smurf2-UbDha adduct.

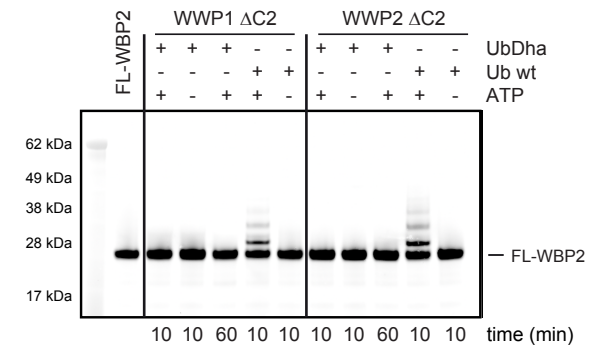

Supplementary Figure 10. Multiple turnover Ubiquitination on substrate WBP2 does not occur with UbDha.

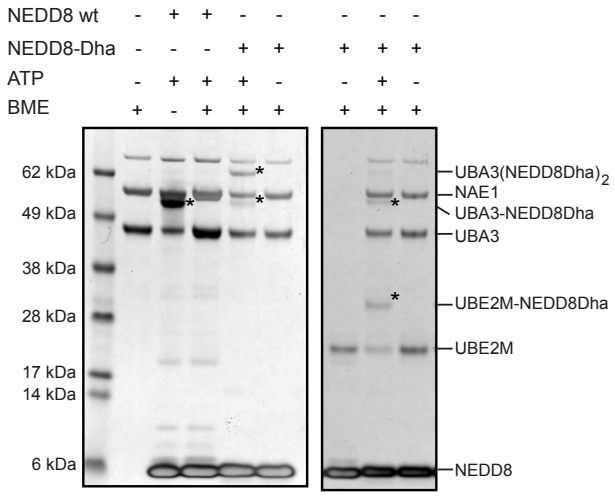

Supplementary Figure 11. NEDD8Dha shows covalent bond formation with the E1 UBA3 and E2 UBE2M (visualized by silver stain). Additionally a higher-running E1 band was detected, presumably corresponding to one NEDD8Dha marking the active site Cys and the other bound to the adenylation domain mimicking an E1 double-loaded intermediate (Supplementary Figure 12). The asterisks indicate the labeled enzyme adducts.

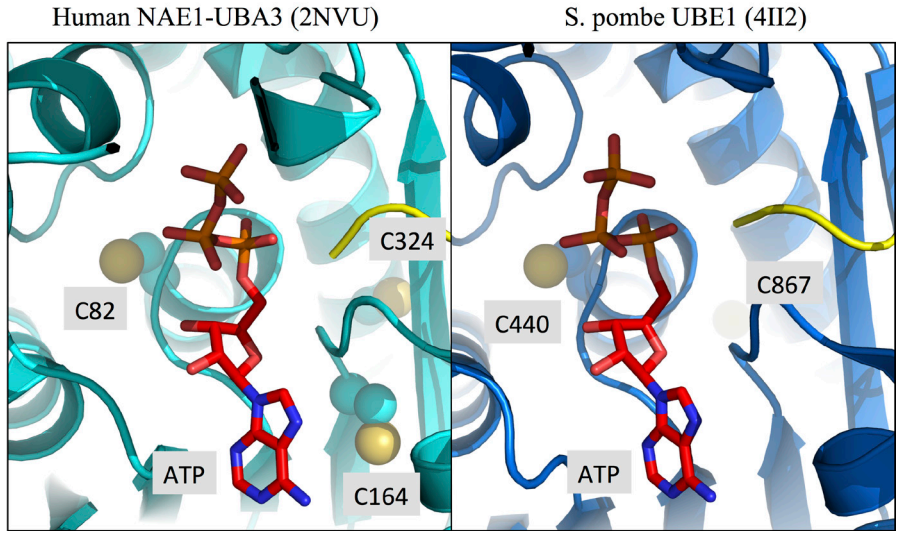

Supplementary Figure 12. Aligned E1 structures of the ATP binding site. The ATP binding site of NAE1 is flanked by three cysteines (Cys82, Cys164 and Cys324)1, one of these (Cys82) is conserved in human UBE1 (Cys481). Note: There is no human E1 crystal structure available. Therefore we used a yeast UBE1 structure2, as a homology model of human UBE1, to present the location of conserved cysteine near ATP (C481 of human UBE1 and C440 of Sp UBE1, human UBE1 and S. pombe share 53.8% sequence identity).

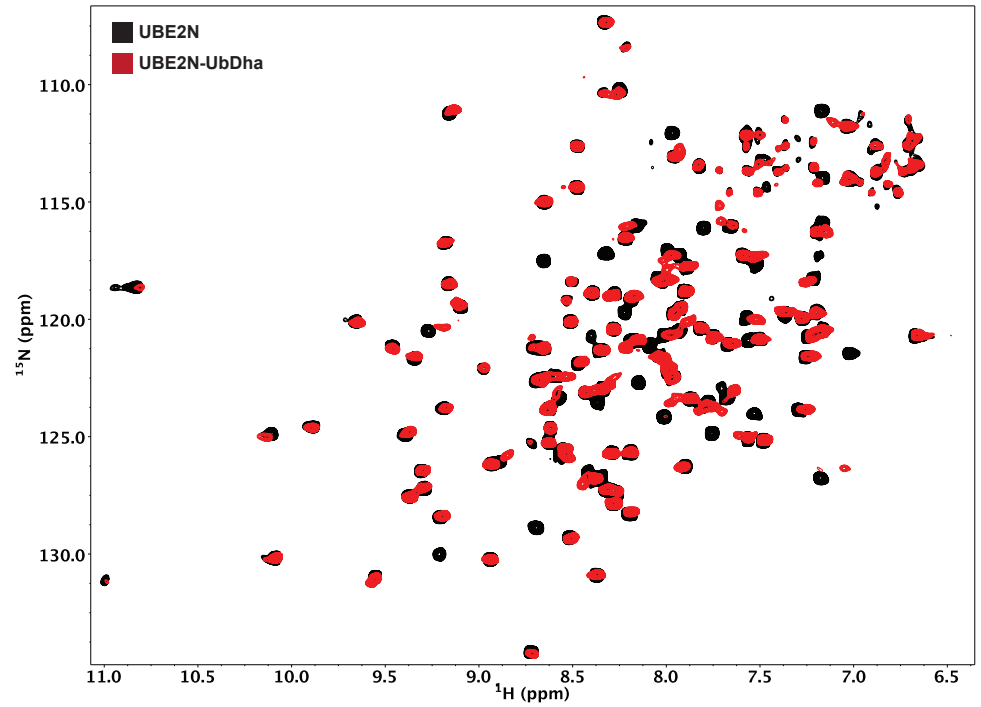

Supplementary Figure 13: Full 1H, 15N HSQC spectra of UBE2N (black) and thioether-linked UBE2N-UbDha (red).

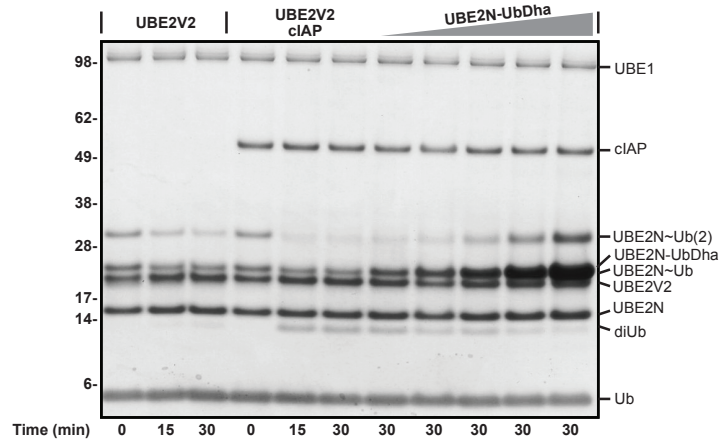

Supplementary Figure 14. Thioether-linked UBE2N-UbDha adduct can compete with downstream Ubiquitination enzymes. Single-turnover Ubiquitination assay monitoring the formation of diUb from thioester-linked UBE2N~Ub. Titration of the stable thioether-linked UBE2N-UbDha into the reaction results in diminished diUb production.

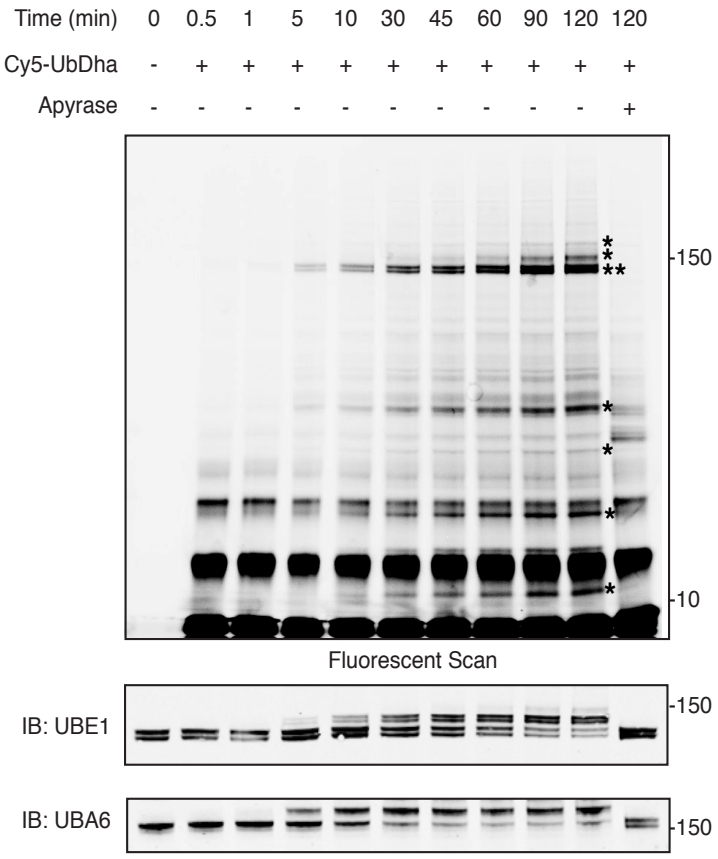

Supplementary Figure 15. Activation of UbDha in cell extracts. Time-course of HeLa cell lysates labeling with Cy5UbDha in the absence (-) or presence (+) of ATP scavenger apyrase. The asterisks indicate ATP-dependent bands.

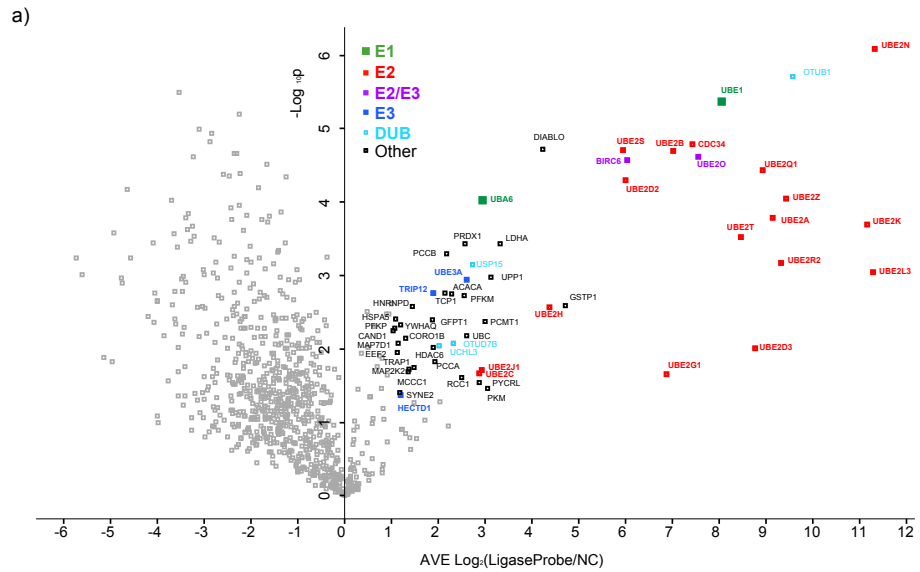

Supplementary Figure 16. Proteome-wide activity profiling of the Ub conjugation machinery in MelJuSo cells. a) Volcano plot of pairwise comparison of proteins bound to the Biotin-UbDha probe relative to the apyrase-treated negative control (negative log10 p-value, y-axis) as a function of average log2 fold enrichment (x-axis). Colored dots represent confidently identified Ubiquitin machinery components as follows: E1 (green), E2 (red), HECT E3 (blue), hybrid E2/E3 (purple) and DUBs (light blue), with an average log2 ratio greater than 1 and with $p < 0.05$. Hits unrelated to the Ub cycle are marked in black, and proteins falling below the threshold are shown in gray. b) Venn diagram of shared Ub-conjugation enzymes recovered from HeLa and MelJuSo cells.

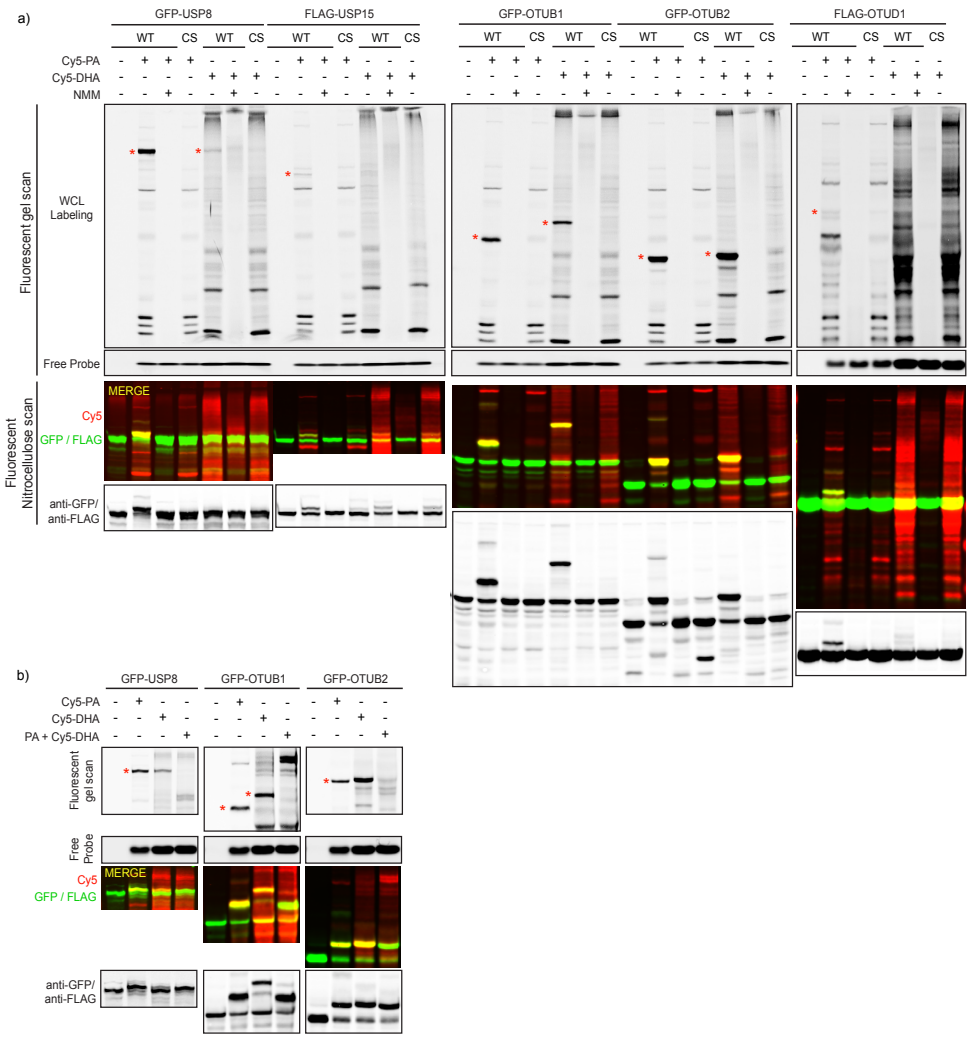

Supplementary Figure 17. DUB labeling: comparison of UbPA and UbDha. Labeling of DUBs in lysates of HEK293T cells transfected as indicated with Cy5-UbPA or Cy5-UbDha, visualized by fluorescence gel scan and immunoblotting against GFP or FLAG. a) Red asterisks indicate labeling of active DUBs. OTUB1 is doubly modified with UbDha, a known characteristic for OTUB1.3 UbPA readily modifies all catalytically competent DUBs tested, while UbDha does not exhibit the same degree of reactivity. Mutations of active-site cysteine residues to serines abolished DUB labeling. b) Labeling of DUBs with Cy5-UbDha was completely abolished upon pretreatment with UbPA.

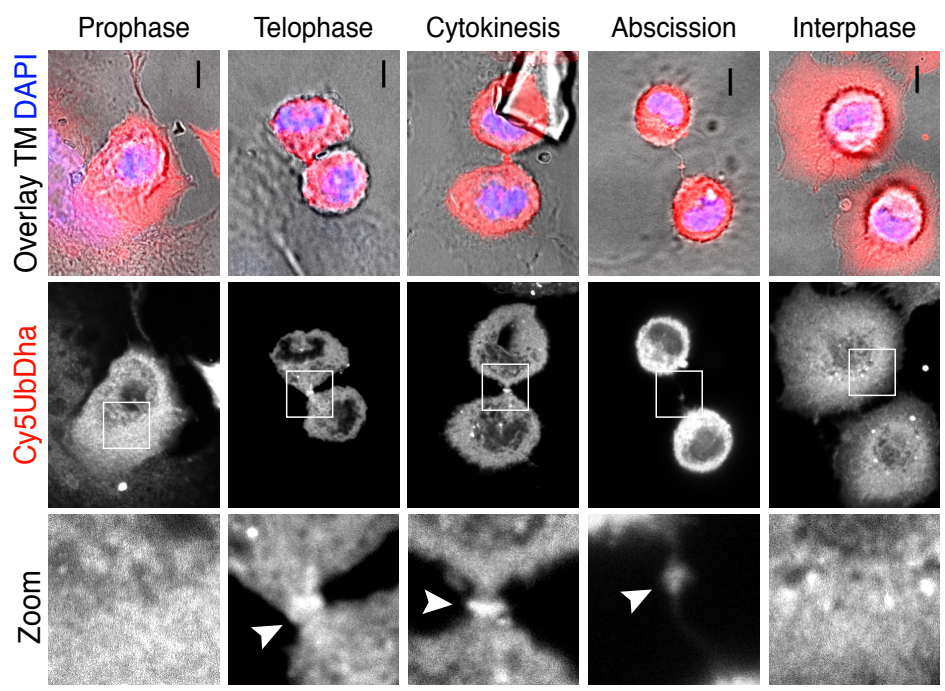

Supplementary Figure 18. Accumulation of Cy5-UbDha probe at the abscission site in diving cells. Cy5-UbDha probe (white, bottom panels) was introduced into HeLa cells by electroporation. Following 1 hr recovery period, cells were fixed and visualized by confocal microscopy. Representative images of cells harboring Cy5-UbDha undergoing various mitotic phases are shown; overlays correspond to Cy5 (red), nuclear DAPI (blue) and the transmission images; scale bars = 5 µm. Arrows point towards the site of abscission, where applicable.